The Plant Cell, Vol. 30: 815–834, April 2018, www.plantcell.org © 2018 ASPB.

Check for updates

EAR1 Negatively Regulates ABA Signaling by Enhancing 2C Protein Phosphatase Activity [OPEN]

Kai Wang,[a,1] Junna He,[a,b,1] Yang Zhao,[c,d] Ting Wu,[a] Xiaofeng Zhou,[a,b] Yanglin Ding,[a] Lingyao Kong,[a] Xiaoji Wang,[a] Yu Wang,[a] Jigang Li,[a] Chun-Peng Song,[e] Baoshan Wang,[f] Shuhua Yang,[a] Jian-Kang Zhu,[c,d] and Zhizhong Gong[a,2]

[a] State Key Laboratory of Plant Physiology and Biochemistry, College of Biological Sciences, China Agricultural University, Beijing 100193, China

[b] College of Horticulture, China Agricultural University, Beijing 100193, China

[c] China Shanghai Center for Plant Stress Biology, Shanghai Institutes of Biological Sciences, Chinese Academy of Sciences, Shanghai 201602, China

[d] Department of Horticulture and Landscape Architecture, Purdue University, West Lafayette, Indiana 47907

[e] Collaborative Innovation Center of Crop Stress Biology, Henan Province, Institute of Plant Stress Biology, Henan University, Kaifeng 475001, China

[f] Key Laboratory of Plant Stress Research, College of Life Science, Shandong Normal University, Ji'nan 250014, China

ORCID IDs: 0000-0003-3681-4340 (J.H.); 0000-0003-1239-7095 (Y.Z.); 0000-0002-3955-7290 (Y.D.); 0000-0002-4395-2656 (J.L.); 0000-0003-3472-8924 (C.-P.S.); 0000-0002-0991-9190 (B.W.); 0000-0003-1229-7166 (S.Y.); 0000-0001-5134-731X (J.-K.Z.); 0000-001-6551-6014 (Z.G.)

The reversible phosphorylation of proteins by kinases and phosphatases is an antagonistic process that modulates many cellular functions. Protein phosphatases are usually negatively regulated by inhibitor proteins. During abscisic acid (ABA) signaling, these inhibitor proteins comprise PYR1/PYL/RCAR ABA receptors, which inhibit the core negative regulators, the clade A type 2C protein phosphatases (PP2Cs). However, it is not known whether these PP2Cs are positively regulated by other proteins. Here, we identified an *Arabidopsis thaliana ear1* (*enhancer of aba co-receptor1*) mutant that exhibits pleiotropic ABA-hypersensitive phenotypes. *EAR1* encodes an uncharacterized protein that is conserved in both monocots and dicots. EAR1 interacts with the N-terminal inhibition domains of all six PP2Cs, ABA INSENSITIVE1 (ABI1), ABI2, HYPERSENSITIVE TO ABA1 (HAB1), HAB2, ABA-HYPERSENSITIVE GERMINATION1 (AHG1), and AHG3, during ABA signaling and enhances the activity of PP2Cs both in vitro and in vivo. ABA treatment caused EAR1 to accumulate in the nucleus. These results indicate that EAR1 is a negative regulator of ABA signaling that enhances the activity of PP2Cs by interacting with and releasing the N-terminal autoinhibition of these proteins.

INTRODUCTION

Reversible protein phosphorylation, a process executed by kinases and phosphatases, is crucial for many eukaryotic cellular processes, including development and growth, the modulation of hormonal inputs, and responses to environmental stimuli (Shi, 2009; Lillo et al., 2014). Ser/Thr phosphatases are a major protein family that can be divided into the protein phosphatase P (PPP) and M (PPM) subfamilies based on sequence similarity (Shi, 2009). The PPP family includes PP1, PP2A, PP2B, PP4, PP5, PP6, and PP7, whereas the PPM family consists of manganese/magnesium ion-dependent phosphatases such as type 2C protein phosphatases (PP2Cs) and pyruvate dehydrogenase phosphatase (Shi, 2009; Lillo et al., 2014). PPP family proteins have both catalytic and regulatory subunits, which include small polypeptide inhibitors in mammals (such as the C-kinase-activated PP1 inhibitor CPI-17 and the PP1 inhibitor I-2) and plants (Arabidopsis inhibitor-2 [AtI-2] and inhibitor-3 [AtInh3]) (Takemiya et al., 2009; Templeton et al., 2011; Eto and Brautigan, 2012). In contrast to the PPP family, PPM family proteins do not have regulatory subunits, but they possess additional domains that determine substrate specificity (Shi, 2009; Lillo et al., 2014).

Plants contain a relatively large number of PP2Cs belonging to the PPM subfamily (Kerk et al., 2008; Shi, 2009), including nine members in clade A PP2C: ABSCISIC ACID (ABA) INSENSITIVE1 (ABI1), ABI2, HYPERSENSITIVE TO ABA1 (HAB1), HAB2, HYPERSENSITIVE GERMINATION1 (AHG1), AHG3, Highly ABA-induced1 (HAI1), AKT1-interacting PP2C1/HAI2, and HAI3 (Koornneef et al., 1984; Leung et al., 1994, 1997; Meyer et al., 1994; Rodriguez et al., 1998; Yoshida et al., 2006; Nishimura et al., 2007; Tischer et al., 2017). These core negative regulators of ABA signaling are inhibited by small PYR1/PYL/RCAR (pyrabactin resistance1/PYR1-like/regulatory component of ABA receptor) ABA receptors (PYLs) (Park et al., 2009; Tischer et al., 2017). In the absence of ABA, PP2Cs interact with and inactivate downstream protein kinases, such as SnRK2s (Snf1-related kinases2), CDPKs (Calcium-dependent protein kinases), CBL/CIPKs (Calcineurin B-like proteins/CBL-interacting proteins), and GHR1 (Guard cell hydrogen

[1] These authors contributed equally to this work.

[2] Address correspondence to gongzz@cau.edu.cn.

The author responsible for distribution of materials integral to the findings presented in this article in accordance with the policy described in the Instructions for Authors (www.plantcell.org) is: Zhizhong Gong (gongzz@cau.edu.cn).

[OPEN] Articles can be viewed without a subscription.

www.plantcell.org/cgi/doi/10.1105/tpc.17.00875

Downloaded from https://academic.oup.com/plcell/article/30/4/815/6099023 by guest on 21 August 2022

IN A NUTSHELL

Background: Abscisic acid (ABA) signaling in plants controls many biological processes, such as seed germination, seedling root growth, and stomatal movement. In the current understanding of ABA signaling, PYR/PYL/RCAR ABA receptor proteins, the clade A type 2C protein phosphatases (PP2Cs), and SNF1-related protein kinase 2s (SnRK2s) constitute the core components of the pathway. In the absence of ABA, PP2Cs negatively regulate ABA signaling by inhibiting the activity of SnRK2s; in the presence of ABA, the PYR/PYL/ACAR ABA receptors bind to and inhibit the phosphatase activity of PP2Cs, thus allowing the activation of SnRK2s and the phosphorylation of their target proteins. The ABA-binding affinities of some PYR/PYL/RCARs are enhanced when they interact with PP2Cs; therefore, PP2Cs are also considered as ABA coreceptors.

Question: In addition to the PYR/PYL/ACAR ABA receptors, are there other components involved in regulating the function of PP2Cs, especially their phosphatase activity?

Findings: We identified a new component named EAR1 (ENHANCER OF ABA CO-RECEPTOR1) that works in concert with clade A PP2C proteins to negatively regulate ABA signaling. The N termini of PP2Cs have a self-inhibition domain to repress their phosphatase activity, while EAR1 can bind to the N-terminal domain of PP2Cs and thus release this self-inhibition effect to enhance their phosphatase activity. Therefore, EAR1 can indirectly inhibit the kinase activity of SnRK2s and ABA signaling. Interestingly, we found that the EAR1 protein was mainly localized on endoplasmic reticulum (ER) in the absence of ABA, whereas ABA treatment induced the translocation of EAR1 from ER to the nucleus. Together, our study identifies EAR1 as a new component of the ABA signaling pathway by interacting with and releasing the N-terminal self-inhibition of PP2Cs.

Next steps: We are exploring the molecular mechanisms regulating ABA-induced translocation of EAR1 from ER to the nucleus. In addition, we are also interested in elucidating the structural changes of PP2Cs in the presence of EAR1.

peroxide-resistant1) (Geiger et al., 2009, 2010; Umezawa et al., 2009; Vlad et al., 2009; Brandt et al., 2012; Hua et al., 2012; Soon et al., 2012), and block ABA signaling. After binding to ABA, PYLs interact with and inhibit PP2Cs, resulting in the activation of downstream protein kinases (Fujii et al., 2009; Park et al., 2009; Cutler et al., 2010). In the absence of ABA, several PYLs, such as PYL5, PYL6, PYL8, PYL9, and PYL10, can still interact with and inhibit PP2Cs, but the inhibition of PP2Cs is weaker than that by ABA-bound PYLs (Hao et al., 2011). However, a subsequent study indicated that the inhibition of PP2Cs by PYL10 depends on ABA (Li et al., 2015), and the previous result demonstrating the inhibition of PP2C by PYL10 in the absence of ABA reflects interference by BSA from the commercial assay kit (Hao et al., 2011). The activated protein kinases phosphorylate their downstream targets, such as ABF transcription factors, to regulate the expression of stress-responsive genes (Furihata et al., 2006; Fujii et al., 2007) or genes encoding ion channels, such as the slow and quick anion channels SLAC1 (Slow anion channel associated1), SLAH3 (SLAC1-homolog protein3), and QUAC1 (Quickly activating anion channel1), thereby modulating stomatal movement (Geiger et al., 2009, 2010; Brandt et al., 2012; Hua et al., 2012). PP2Cs are considered to act as ABA coreceptors, as they enhance the strength of ABA binding by PYLs (Melcher et al., 2009; Park et al., 2009; Yin et al., 2009).

In addition to inhibition by ABA-bound PYLs, ABI1 is regulated by PUB12/13 U-box E3 ligase-mediated protein degradation (Kong et al., 2015). Interestingly, the ubiquitination of ABI1 occurs only after this protein interacts with PYLs, either in the presence (such as PYR1) or absence (such as PYL4 and PYL9) of ABA (Kong et al., 2015). In this study, we identified a previously uncharacterized gene, *Enhancer of ABA Co-Receptor1* (*EAR1*), during a genetic screening for mutants with ABA-inhibited primary root growth. The *ear1* mutants are hypersensitive to ABA during all ABA responses. Genetic and biochemical analyses indicated that EAR1 interacts with the N termini of the six PP2Cs in *Arabidopsis thaliana* during ABA signaling and enhances their activity. However, this interaction does not affect the inhibition of PP2Cs by PYLs. These results identify a mechanism for the regulation of PP2Cs through their interaction with EAR1.

RESULTS

EAR1 Is a Negative Modulator of ABA Signaling

To isolate uncharacterized ABA-responsive mutants, we performed forward genetic screening with an ethyl methanesulfonate-mutagenized M2 population using ABA-induced inhibition of primary root growth for screening (Wang et al., 2011a). One mutant, *ear1-1*, was isolated. We backcrossed *ear1-1* with the wild type four times before performing the following analyses. Primary root growth was determined after 5-d-old seedlings were moved from Murashige and Skoog (MS) medium to MS medium containing different concentrations of ABA. There was no difference in primary root growth between *ear1-1* and the wild type when the plants were grown on MS medium. However, ABA inhibited primary root growth to a greater extent in *ear1-1* than in wild-type plants (Figures 1A and 1B). We also investigated the sensitivity of *ear1-1* to ABA during seed germination on MS medium. With increasing concentrations of ABA in the medium, the seed germination greening ratio of *ear1-1* became increasingly significantly reduced compared with the wild type (Figures 1C and 1D). Under these ABA concentrations, almost all wild-type seedlings became green after 7 d. As a control, we examined the germination greening ratio on MS medium and found no difference between

Downloaded from https://academic.oup.com/plcell/article/30/4/815/6099023 by guest on 21 August 2022

ear1-1 and the wild type. We also tested the drought tolerance of seedlings grown in soil. After withholding water for 14 d, the leaves of 21-d-old *ear1-1* plants appeared to be healthier than those of the wild type. After 3 d, the seedlings were watered and allowed to recover (Figure 1E). Nearly 100% of the *ear1-1* plants survived, whereas all of the wild-type plants died. Water loss analysis in detached leaves demonstrated that the rate of water loss was much slower in *ear1-1* than in the wild type at various time points (Figure 1F). These results demonstrate that EAR1 is a general negative regulator of ABA signaling that functions in seed germination, primary root growth, and drought tolerance.

EAR1 Encodes a Previously Uncharacterized Protein

To clone the *EAR1* gene, we crossed the *ear1-1* mutant in the Col-0 background with wild-type plants of the Landsberg *erecta* accession. Five-day-old F2 seedlings grown on MS medium were transferred to MS medium supplemented with 30 μM ABA. After 5 d, we selected putative mutants based on hypersensitivity of root growth to ABA and subjected them to map-based cloning with simple sequence length polymorphism (SSLP) markers. *EAR1* was localized between BAC clones F13M11 and MWD9 on chromosome 5 (Figure 2A). We sequenced the open reading frames of all candidate genes between the two SSLP markers and identified a C163-to-T substitution in *AT5G22090* (counting from the first putative ATG initiation codon). This point mutation created a premature stop codon, resulting in a truncated putative peptide of 54 amino acids. We obtained a T-DNA insertion line for this gene (SALK_057606, *ear1-2*) from the Arabidopsis Stock Center. The T-DNA was inserted at position 1088 of *AT5G22090* and did not alter its transcript size before the T-DNA insertion (Figure 2A; Supplemental Figures 1A and 1B). However, *ear1-2* exhibited a similar ABA-sensitive phenotype to the wild type (Supplemental Figure 1C), indicating that the T-DNA insertion did not disrupt the biological function of *AT5G22090* in *ear1-2* (see below for detailed analyses of the transgenic plants). We also constructed a CRISPR/Cas9 line, *ear1-c*, using an egg cell-specific editing system (Wang et al., 2015). The *ear1-c* mutant has a 1-bp insertion at position 476 bp (counting from the first putative ATG initiation codon) that would create a stop codon after 177 amino acids due to a frame shift (Supplemental Figure 1D). The roots of the *ear1-c* mutant showed a similar level of hypersensitivity to ABA as those of *ear1-1* (Supplemental Figure 1E).

EAR1 cDNA was obtained via RT-PCR. *EAR1* encodes an uncharacterized protein of 463 amino acids. The Arabidopsis genome contains only one copy of *EAR1*. Database searches indicated that EAR1 homologs are highly conserved in land plants, with more homologs occurring in dicots than in monocots (Supplemental Figures 2A and 2B and Supplemental Data Set 1). The EAR1 homologs contain two highly conserved regions. The first region is located from amino acid 133 to 167, with one KSLE and one CTESLG motif, and the second is located from amino acid 224 to 278, with two GRL motifs (this protein is a DUF3049 family protein based on these two regions) (Supplemental Figure 2B). To confirm that the *ear1-1* mutant harbors a mutation in *EAR1*, we constructed a binary vector containing a 2332-bp promoter sequence (*EAR1* native promoter) driving *EAR1* cDNA and introduced this vector into *ear1-1* via *Agrobacterium tumefaciens*-mediated transformation. We selected two representative lines that showed similar levels of ABA sensitivity to that of the wild type (Figure 2B). GUS staining of transgenic seedlings carrying *ProEAR1:GUS* indicated that *EAR1* was constitutively expressed in most tissues, including 2-d-old seedlings and guard cells (Figure 2C).

The EAR1$^{141-287}$ Fragment Is Sufficient for the Functioning of EAR1 in ABA Responses

Since disrupting the C terminus of EAR1 did not affect its function (as shown in the *ear1-2* T-DNA insertion mutant in Supplemental Figure 1C), we investigated which region is crucial for its function. We generated serial deletion mutants of *EAR1* and transferred them (under the control of the *EAR1* native promoter) into *ear1-1* plants to assess which region could complement the ABA hypersensitivity phenotype of *ear1-1*. Fragments containing EAR1$^{141-287}$ were able to complement the ABA hypersensitive phenotype of *EAR1* during primary root growth (Figure 2D). These results demonstrate that the EAR1$^{141-287}$ fragment is sufficient for the functioning of EAR1 in ABA responses.

EAR1 Mutation Enhances the ABA Response in Core ABA Signaling Mutants

To analyze the genetic relationship between *EAR1* and other ABA signaling components, we crossed *ear1-1* with various PP2C and SnRK2 mutants. The *abi1-2/abi2-1/hab1-1* triple loss-of-function mutant (*3m*) is hypersensitive to ABA during seed germination and root growth (Rubio et al., 2009). An ABA concentration of 20 nM inhibited the germination of the *ear1-1/abi1-2/abi2-2/hab1-1* quadruple mutant (*4m*) but not the *3m* or *ear1-1* mutant (Figures 3A and 3B). Similarly, 3 μM ABA treatment arrested root growth in most *4m* seedlings (Figure 3C) compared with 10 μM ABA for *3m* seedlings and 30 μM ABA for *ear1-1* (Figure 3C). We also assessed the drought phenotypes of seedlings grown in soil. We withheld water from 2-week-old seedlings grown in soil and assessed their growth status. After watering was withheld, leaf wilting first appeared in wild-type seedlings, followed by *ear1-1*, *3m*, and finally *4m*, indicating that *4m* is more tolerant to drought stress than *3m* (Figure 3D).

Leaf temperature reflects the strength of transpiration, with a high leaf temperature indicating low levels of transpiration. The lines with the lowest to highest leaf temperature were as follows: the wild type, *ear1-1*, *3m*, and *4m* (Figures 3E and 3F). These results indicate that *4m* is more sensitive to ABA during seed germination and root growth and more tolerant to drought stress than *3m* and *ear1-1*. The *snrk2.2/snrk2.3* double mutant shows strong ABA-insensitive phenotypes during seed germination (Fujii et al., 2007). The *ear1-1/snrk2.2/snrk2.3* triple mutant was more sensitive to ABA than was *snrk2.2/snrk2.3* but less sensitive than the wild type or *ear1-1* during seed germination (Figures 3G and 3H). These results further suggest that EAR1 is a general negative modulator of the ABA signaling pathway.

Transgenic Plants Overexpressing EAR1 Are Less Sensitive to ABA Than Are Wild-Type Plants

We overexpressed *EAR1-Flag* under the control of the *35S* promoter and selected two transgenic lines (*OE-16*$^{\#}$ and *OE-28*$^{\#}$) that

Downloaded from https://academic.oup.com/plcell/article/30/4/815/6099023 by guest on 21 August 2022

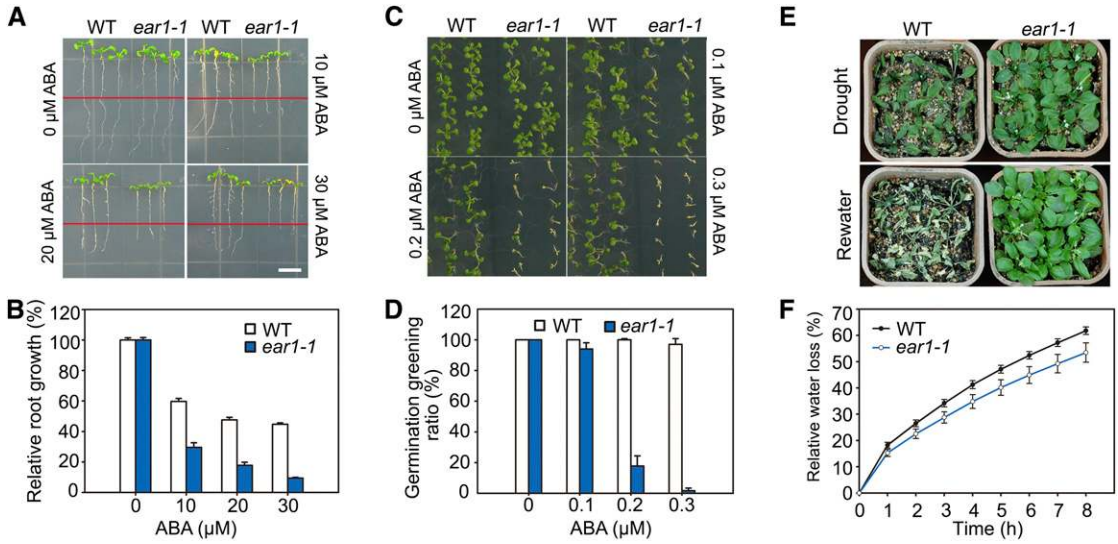

Figure 1. *ear1-1* Is Sensitive to ABA.

(A) Primary root growth in *ear1-1* is sensitive to ABA. Wild-type (WT) and *ear1-1* seeds were germinated on MS medium and grown for 5 d before being transferred to MS medium containing different concentrations of ABA. Bar = 1 cm.

(B) Statistical analysis of relative root growth of *ear1-1* and the wild type in **(A)**. The absolute root length in the wild type and *ear1-1* on MS medium was set to 100%. Bars are means ± SE of nine seedlings from three plates. Three different experiments were performed with similar results.

(C) Seed germination in *ear1-1* is sensitive to ABA. The seeds were germinated on MS medium containing different concentrations of ABA for 7 d.

(D) The germination greening ratio in **(C)**. Bars are means ± SE of three biological replicates. Approximately 40 seeds were analyzed in each replicate. The greening ratios did not show a clear difference in the wild type under these concentrations.

(E) Soil-grown *ear1-1* seedlings are more drought tolerant than the wild type. Twenty-one-day-old seedlings were subjected to drought stress by withholding water for 14 d. The plants were photographed before and after rewatering.

(F) Relative water loss in the wild type and *ear1-1*. Four-week-old plants were used for water loss measurements in detached leaves. Data are means ± SE of three replicates (15 leaves from one pot were measured per replicate) in one experiment. Three independent experiments were performed, with similar results.

showed higher EAR1 levels than two other lines (Figure 4A) to investigate the effect of EAR1 on ABA responses. There was no clear morphological difference among wild-type, *ear1-1*, *OE-16*#, and *OE-28*# seedlings grown in soil (Supplemental Figures 3A to 3C). The seed germination greening ratio was highest in *OE-16*# and was higher in *OE-28*# than in the wild type, whereas the lowest seed germination greening ratio was observed in *ear1-1* (Figure 4B; Supplemental Figure 3D). Root growth was most resistant to ABA in *OE-16*#, more resistant to ABA in *OE-28*# than in the wild type, and most sensitive to ABA in *ear1-1* (Figures 4C and 4D).

We also compared ABA-mediated stomatal movement among these genotypes. We treated epidermal peels from different genotypes with MES buffer in the light to fully open the stomata and added 20 μM ABA to the buffer. After 2 h, we measured stomatal apertures. Treatment with 20 μM ABA reduced the stomatal aperture to the greatest extent in *ear1-1*, to a greater extent in the wild type than in the overexpressing mutant *OE-28*#, and to the lowest extent in *OE-16*# (Figure 4E). We also investigated the effect of ABA on inhibiting light-promoted stomatal opening, finding that the light-induced opening of stomata that had closed in the dark was inhibited by ABA to the greatest extent in *ear1-1* and to a greater extent in the wild type than in *OE-16*# or *OE-28*# (Figure 4F). *OE-16*# exhibited the lowest leaf temperatures among the four genotypes, and *ear1-1* showed the highest leaf temperature (Figures 4G and 4H). Detached leaves of *OE-16*# and *OE-28*# lost more water than those of the wild type, which lost more water than those of *ear1-1* (Figure 4I). Consistently, *ear1-1* had the lowest transpiration rate, whereas that of *OE-16*# was the highest (Figure 4J). We also compared drought tolerance among EAR1-overexpressing transgenic plants, wild-type plants, and *ear1-1* plants. After withholding water, leaf wilting first appeared in *OE-16*# seedlings, followed by *OE-28*#, then the wild type, and finally *ear1-1*, indicating that *OE-16*# and *OE-28*# were less tolerant to drought stress than was the wild type, and *ear1-1* was the most tolerant to drought stress among the genotypes (Figure 4K). These results indicate that EAR1 is a general negative modulator of ABA signaling.

EAR1 Interacts with PP2Cs

PP2Cs and SnRK2.2/2.3/2.6 (OST1) are central negative and positive regulators, respectively, of the early ABA signaling pathway, and PYLs act as inhibitors of PP2Cs. As *ear1-1* was hypersensitive to ABA in all ABA responses examined, we reasoned that EAR1 might interfere with early ABA signaling components by positively regulating PP2Cs, negatively regulating SnRK2.2/2.3/OST1, or negatively regulating PYLs. Therefore, we performed a bimolecular fluorescence complementation (BiFC)

Downloaded from https://academic.oup.com/plcell/article/30/4/815/6099023 by guest on 21 August 2022

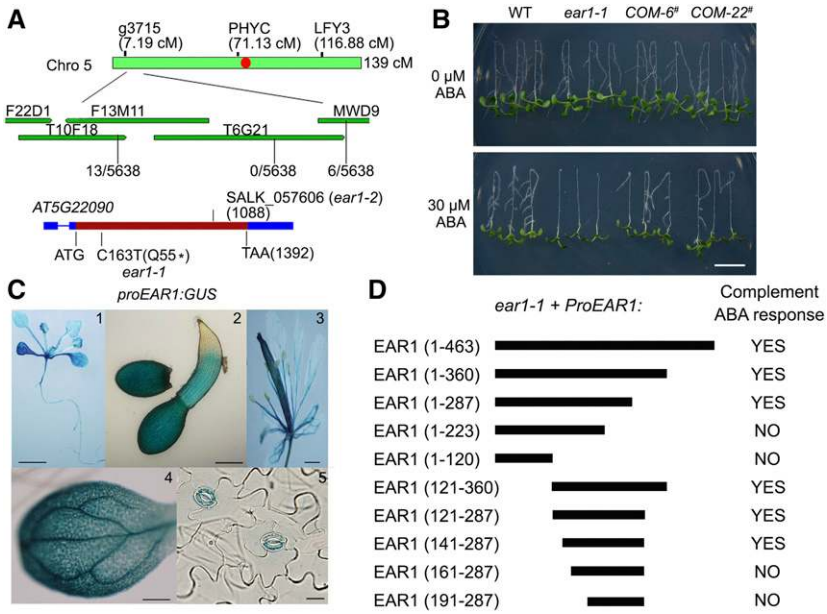

Figure 2. Cloning and Complementation of *EAR1*.

(A) Mapping-based cloning of *EAR1*. The *EAR1* locus was mapped to the top of chromosome 5 and narrowed down to BAC clones T10F18 and MWD9 using a total of 2819 samples. A G-to-A mutation in position 163 and a T-DNA insertion at position 1088 in *AT5G22090* are indicated. The red dot represents the centromere of chromosome 5.
(B) The ABA-sensitive root growth of *ear1-1* is complemented by *EAR1*. The *EAR1* genomic sequence fused with *GFP* was used to generate the transgenic complemented lines; two independent lines (*COM-6* and *COM-22*) were used for phenotype analysis on MS medium containing 30 μM ABA. Bar = 1 cm.
(C) *ProEAR1:GUS* expression patterns in different tissues, including a 7-d-old whole seedling (1), 2-d-old young seedling (2), flower (3) mature leaf (4), and guard cells (5). Bar in (1) = 1 cm, bar in (2) = 200 μm, bar in (3) = 1 mm, bar in (4) = 2 mm, and bar in (5) = 20 μm.
(D) Complementation of *ear1-1* by fragments not shorter than EAR1$^{141-287}$. Different deletion forms of *EAR1* were constructed and expressed under the control of the *EAR1* native promoter in *ear1-1*. ABA sensitivity of root growth was examined in these transgenic plants grown on MS medium containing 30 μM ABA. YES, complemented the root ABA-hypersensitive phenotype of *ear1-1*; NO, did not complement the root ABA-hypersensitive phenotype of *ear1-1*.

assay (Walter et al., 2004) to determine whether EAR1 interacts with different core components involved in ABA signaling. We found that EAR1-cYFP physically interacted with ABI1-, ABI2-, HAB1-, HAB2-, AHG1-, and AHG3-nYFP (Figure 5A) but not with three other PP2Cs, HAI1, AKT1-interacting PP2C1/HAI2, and HAI3 (Supplemental Figure 4A), in *Nicotiana benthamiana* leaf transient assays performed via Agrobacterium infiltration. HAI mutants exhibit more ABA-independent low water potential phenotypes than mutants with the classical ABA-sensitive phenotypes (Bhaskara et al., 2012). However, HAIs are also regulated by all PYLs (Tischer et al., 2017). We also subjected Arabidopsis protoplasts transiently coexpressing EAR1-Flag with ABI1-, ABI2-, HAB1-, HAB2-, AHG1-, or AHG3-Myc to coimmunoprecipitation (co-IP) assays. The co-IP assays indicated that all of the MYC-tagged PP2Cs coimmunoprecipitated EAR1-Flag (Figure 5B).

We also used Flag beads to immunoprecipitate proteins extracted from 14-d-old EAR1-Flag transgenic seedlings treated with 60 μM ABA for 3 h or no ABA treatment. Immunostaining assays with anti-ABI1 and -ABI2 antibodies showed that EAR1-Flag coimmunoprecipitated both ABI1 and ABI2 (Figure 5C). Like ABI1 antibodies (Kong et al., 2015), ABI2 antibodies were relatively specific (Supplemental Figure 4B). We also analyzed the immunoprecipitated proteins by liquid chromatography-tandem mass spectrometry (LC-MS/MS) (Kong et al., 2015). We identified ABI1 and HAB2 from the no-ABA-treatment sample and ABI1 and AHG3 from the ABA-treated sample (Supplemental Data Sets 2 and 3), suggesting that EAR1-Flag coimmunoprecipitated ABI1, HAB2, and AHG3. Finally, we performed protein pull-down assays to analyze the physical interaction of EAR1 with the PP2Cs. We expressed each of these proteins fused with different tags in *Escherichia coli* and isolated the resulting proteins from *E. coli*. Protein pull-down assays indicated that MBP-ABI1 or MBP-ABI2, but not MBP, was able to pull down EAR1$^{121-287}$-His (Figure 5D), whereas HAB1-His, HAB2-His, AHG1-His, and AHG3-His only pulled down GST-EAR1$^{121-287}$ but not the negative control GST (Supplemental Figure 4C). These results indicate that EAR1 physically interacts with these PP2Cs both in plant cells and in vitro.

To determine which region of EAR1 interacts with these PP2Cs, we assessed the interactions of different EAR1 fragments with one representative PP2C, ABI1, via BiFC assays. We found that the N terminus (1 to 120) and C terminus (288 to 463) of EAR1 did not interact with ABI1, but the middle region containing EAR1$^{191-287}$ did interact with ABI1 (Figure 5E). Further deletion analysis indicated that EAR1$^{191-287}$ interacted with the N terminus (1 to 130), but not the C terminus (131 to 434), of ABI1 (Figure 5E), whereas

Downloaded from https://academic.oup.com/plcell/article/30/4/815/6099023 by guest on 21 August 2022

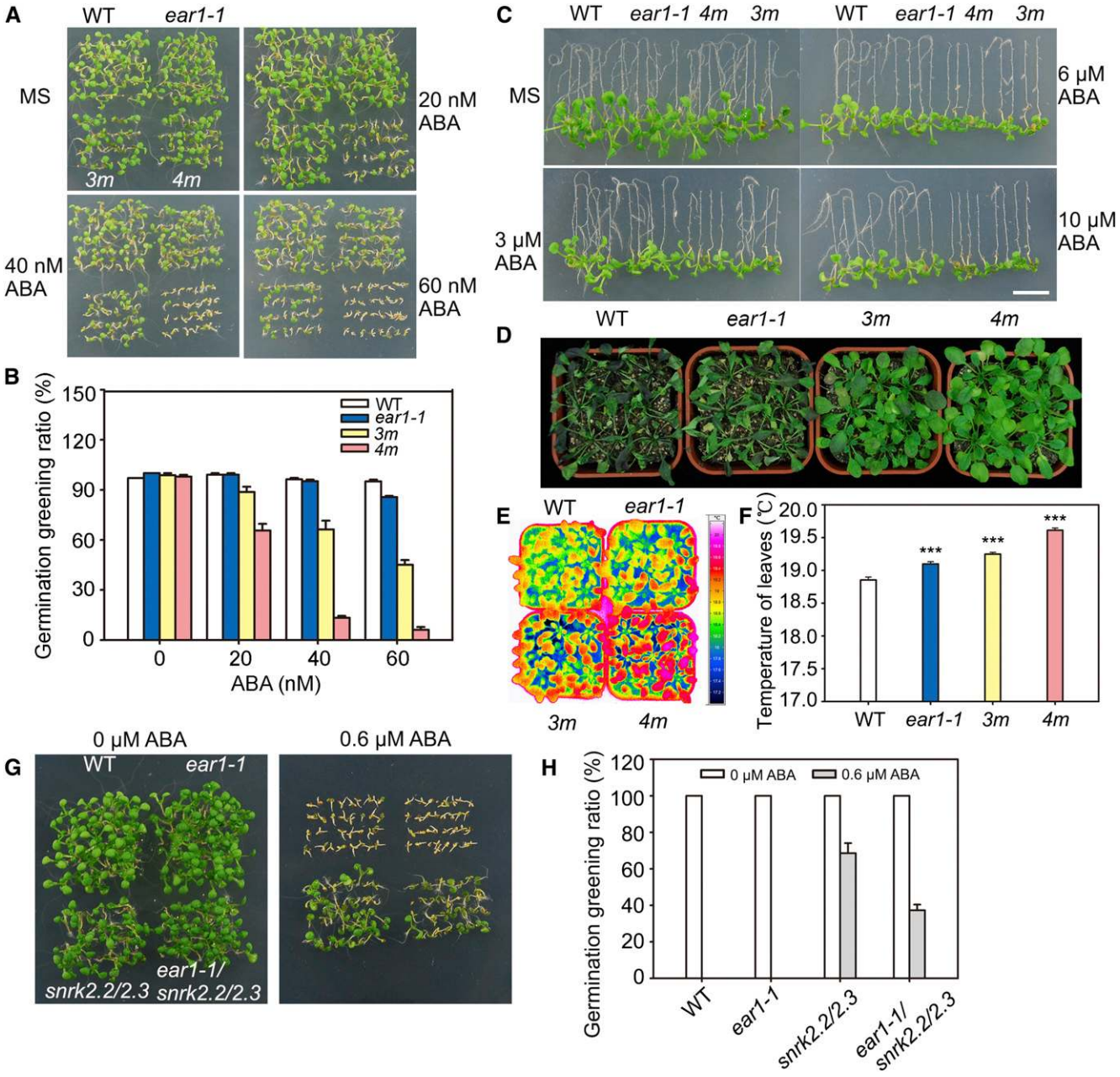

Figure 3. Genetic Analysis of *ear1-1* with the Clade A *pp2c* and *snrk2* Mutants.

(A) Germination phenotypes of the wild type, *ear1-1*, *3m*, and *4m* on MS medium containing different concentrations of ABA. The seed germination of *4m* was more sensitive to ABA compared with that of *ear1-1* and *3m*.

(B) Seed germination greening ratio in **(A)**. Bars are means ± SE of three experiments. Approximately 40 seeds were analyzed in each experiment.

(C) Root growth phenotypes of the wild type, *ear1-1*, *3m*, and *4m* on MS medium containing different concentrations of ABA. Primary root growth of *4m* was more sensitive to ABA compared with that of *ear1-1* or *3m*. Bar = 1 cm.

(D) *4m* is more drought tolerant than *ear1-1* and *3m*. Three-week-old seedlings grown under normal conditions were subjected to drought stress by withholding water for 2 weeks before being photographed.

(E) Leaf temperature in the wild type, *ear1-1*, *3m*, and *4m*. The seedlings were grown under normal conditions for 21 d, and water was withheld for 7 d before measurement.

(F) Statistical analysis of leaf temperatures in **(E)**. Bars are means ± SE of three replicates (15 leaves from one pot were measured per replicate, and three different pots were analyzed). The asterisks indicate significant differences compared with the wild type treated with ABA (***$P < 0.005$, Student's *t* test).

Downloaded from https://academic.oup.com/plcell/article/30/4/815/6099023 by guest on 21 August 2022

EAR1$^{121-248}$ and EAR1$^{249-278}$ did not interact with ABI1 (Supplemental Figure 4D). The ABI1 N terminus is an autoinhibition domain (Sheen, 1998). The N termini are not conserved in clade A PP2Cs. To determine whether the N termini of the other PP2Cs interact with EAR1, we performed BiFC assays and confirmed that the N terminus of ABI2$^{1-120}$-, HAB1$^{1-200}$-, HAB2$^{1-200}$-, AHG1$^{1-200}$-, and AHG3$^{1-120}$-nYFP, but not the C-terminal catalytic domains, interacted with EAR1-cYFP (Supplemental Figure 4E). These results demonstrate that EAR1 interacts with the N termini of all six clade A PP2Cs.

EAR1 Enhances the Activity of PP2Cs

EAR1 is a negative regulator of ABA signaling that interacts with the inhibition domain at the N termini of PP2Cs. Hence, it is possible that EAR1 releases the autoinhibition activity of ABI1. To test this hypothesis, we measured ABI1 activity in vitro in the presence of EAR1. In agreement with the results of transgenic analysis, removing the EAR1 N terminus did not affect its function in complementing the *EAR1* mutant; therefore, we expressed EAR1 without the N terminus (1 to 120) in *E. coli* (when amino acids 1 to 120 were included, the construct was difficult to express) and ABI1 (Supplemental Figure 5A). The addition of EAR1$^{121-287}$ increased the activity of ABI1 in vitro (Figure 6A). ABA-bound PYR1 greatly inhibited the activity of ABI1 (Figure 6A). However, the addition of EAR1$^{121-287}$ did not appear to alter the receptor-mediated inhibition of ABI1, and it still enhanced ABI1 activity (Figure 6A), suggesting that EAR1 somehow interferes with PYR1-induced inhibition or enhances the activity of free ABI1 released from the PYR1-ABA-ABI1 complex. Further assays with the five other PP2Cs showed that EAR1$^{121-287}$ enhanced the phosphatase activity of all these proteins (Figure 6B) but had no effect on calf intestinal alkaline phosphatase activity (Figure 6B) or other representative PP2Cs that did not belong to clade A (Figure 6C). A kinetic-dependent assay of ABI1 phosphatase activity indicated that the K_m of ABI1 with or without EAR1 was 18.6 or 20.8 μM, respectively (Figure 6D). ABI1 activity increased with increasing concentrations of EAR1$^{121-287}$ (Supplemental Figure 5B). We also measured ABI1 activity in the absence or presence of EAR1 mixed with the phosphopeptide substrate for 0 to 90 min. ABI1 used the substrate more quickly in the presence of EAR1 than in its absence (Supplemental Figure 5C).

To investigate whether EAR1 interferes with the interaction between PYR1 and ABI1, we performed protein pull-down and yeast three-hybridization assays. These assays indicated that EAR1 does not affect the interaction of PYR1 with ABI1 (Supplemental Figures 6A and 6B). ABI1 is degraded by PUB12/13 in the presence of ABA (Kong et al., 2015). In this study, a protein degradation assay indicated that ABI1 was degraded at a similar level in the wild type and the *ear1-1* mutant (Supplemental Figure 6C).

Analysis of the EAR1 amino acid sequence using PONDR (Predictor Of Natural Disordered Regions; http://www.pondr.com/) indicated that EAR1$^{131-248}$ harbors an intrinsically disordered region (IDR; proteins containing IDRs are referred to as intrinsically disordered proteins [IDPs]), and only EAR1$^{249-278}$ can form a predicted regular structure (Supplemental Figure 7A). The apparent molecular weight of EAR1 observed in a gel was ~2 times greater than its theoretical molecular weight (Figures 4A and 5C), suggesting that it is not a monomeric, globular protein but is most likely a polypeptide chain of natively unfolded or intrinsically unstructured proteins. Interestingly, PONDR predicted that the N termini of five A-type PP2Cs, ABI1, ABI2, HAB1, HAB2, and AHG3, contain an IDR, and the N terminus of AHG1 likely forms an IDR because the ability of this region to form an ordered structure is relatively weak (Supplemental Figure 6A). It appears that HAI1, HAI2, and HAI3 do not form clear IDRs (Supplemental Figure 7A). Using MoRFpred (http://biomine-ws.ece.ualberta.ca/MoRFpred/index.html, http://anchor.enzim.hu/) (Mészáros et al., 2009; Disfani et al., 2012), we detected some putative MoRFs (molecular recognition features, labeled in red) in the N termini of all six PP2Cs (Supplemental Figure 7B). To investigate whether these MoRFs play crucial roles in protein interactions, we produced several truncated peptides lacking one or more MoRFs. BiFC assays indicated that ABI$^{1-100}$ lacking the last MoRF or ABI$^{100-130}$ containing the last MoRF, ABI2$^{29-100}$ lacking the first two and last MoRF or ABI2$^{90-120}$ containing the last MoRF, HAB2$^{1-96}$ lacking the last two MoRFs or HAB2$^{96-200}$containing the last MoRF, AHG1$^{1-116}$ lacking the last two MORFs or AHG1$^{116-200}$ containing the last two MoRFs, and AHG3$^{1-42}$ containing the first two MoRFs or AHG3$^{42-120}$ lacking the first two MoRFs fused with nYFP did not interact with EAR1-cYFP. By contrast, HAB1$^{21-200}$ lacking the first MoRF fused with nYFP did interact with EAR1-cYFP (Supplemental Figure 7C). However, neither HAB1$^{21-129}$ lacking the last MoRF nor HAB1$^{129-200}$ containing the last MoRF interacted with EAR1. These results indicate that some putative MoRFs and/or peptide length are important for their interaction with EAR1.

Removing the N terminus (1 to 120) of ABI1 significantly increased its phosphatase activity (Supplemental Figure 7D), which is consistent with the previous finding that the N terminus is an autoinhibition domain (Sheen, 1998). However, the addition of EAR1$^{121-287}$ did not further increase the activity of ABI1$^{121-434}$ (Supplemental Figure 7D), suggesting that EAR1 increases ABI1 activity by inhibiting the N terminus of ABI1. Based on the MoRF prediction and the above protein interaction results, we further analyzed the EAR1-enhanced activity of ABI2 and AHG3. As shown in Figure 6E, removing 28 amino acids from the N terminus of ABI2 did not affect the interaction of ABI2 with EAR1 (Supplemental Figure 7D), and it did not affect EAR1-enhanced ABI2 activity. Importantly, removing 42 amino acids from AHG3 eliminated its interaction with EAR1 (Supplemental Figure 7D), and

Figure 3. (continued).

(G) Seed germination phenotypes of the wild type, *ear1-1*, *snrk2.2/snrk2.3* (*snrk2.2/2.3*), and *ear1-1/snrk2.2/snrk2.3* (*ear1-1/snrk2.2/2.3*). Seeds were germinated on MS medium with or without 0.6 μM ABA for 7 d.

(H) Seed germination greening ratios of plants in **(G)**. Bars are means ± SE of three experiments. Approximately 40 seeds were analyzed in each experiment. The insensitivity of *snrk2.2/snrk2.3* to ABA-inhibited germination was compromised by the *ear1-1* mutation.

Downloaded from https://academic.oup.com/plcell/article/30/4/815/6099023 by guest on 21 August 2022

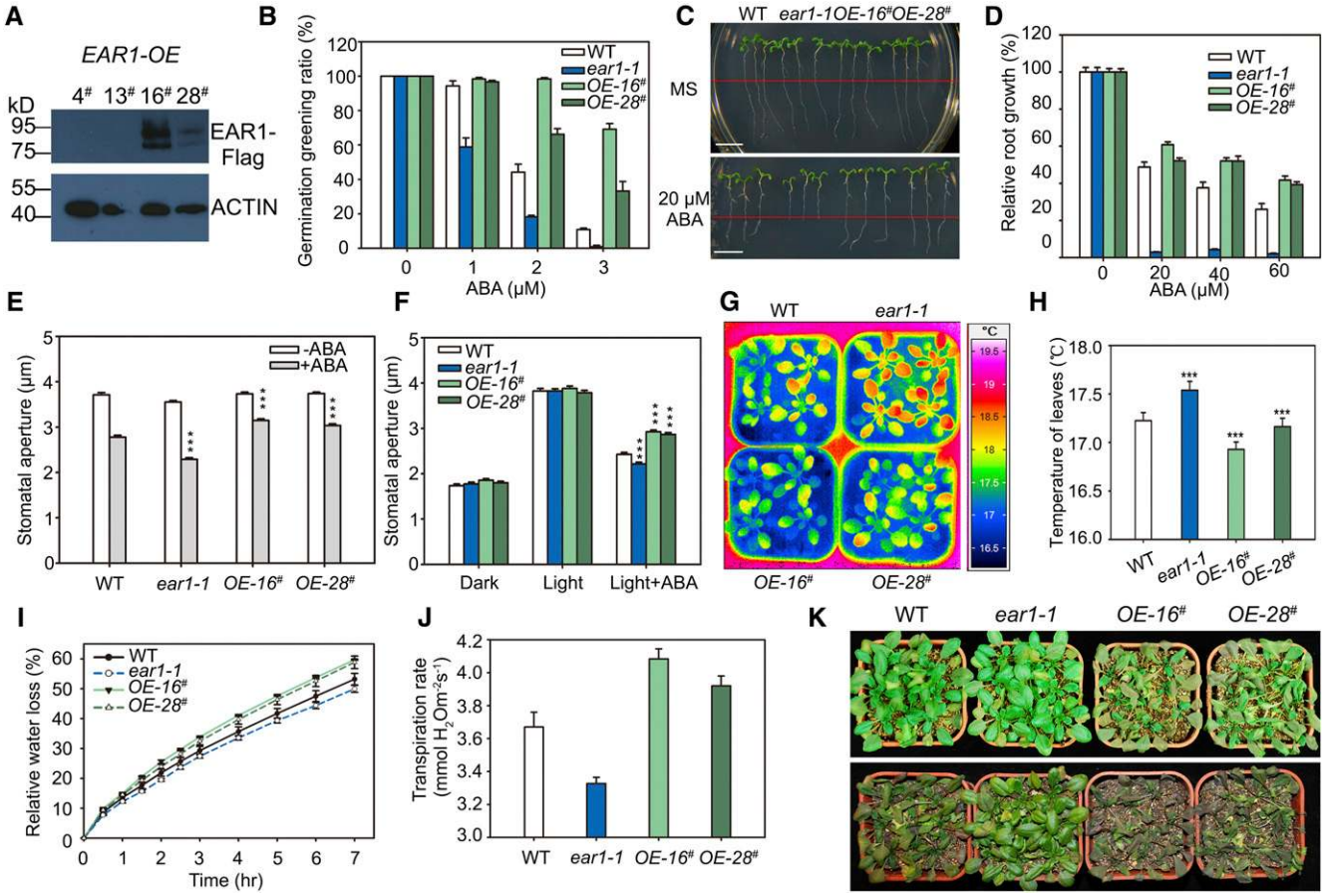

Figure 4. Overexpression of *EAR1* Enhances Plant Resistance to ABA.

(A) EAR1-Flag levels in transgenic lines 4#, 13#, 16#, and 28# determined by immunoblotting using anti-Flag antibodies. ACTIN was used as a loading control.
(B) Seed germination greening ratios of the wild type, *ear1-1*, *OE-16#*, and *OE-28#*. Seeds were germinated on MS medium containing different concentrations of ABA. Bars are means ± SE of three biological replicates. Approximately 40 seeds were analyzed per replicate.
(C) Primary root growth phenotypes of the wild type, *ear1-1*, *OE-16#*, and *OE-28#*. Seeds were germinated on MS medium and grown for 5 d before being transferred to MS medium or MS medium containing 20 μM ABA. Bar = 1 cm.
(D) Relative primary root growth of plants shown in **(D)**. The absolute root length of the wild type and *ear1-1* on MS medium was set to 100%. Bars are means ± SE of three replicates, each replicate with three seedlings. Three experiments were performed, with similar results.
(E) ABA-promoted stomatal closure in the wild type, *ear1-1*, *OE-16#*, and *OE-28#*. Epidermal strips with fully open stomata were treated with or without 20 μM ABA for 2 h before being photographed. Bars are means ± SE of three biological replicates (20 stomata from one seedling per replicate). The asterisks indicate significant differences compared with the wild type treated with ABA (***P < 0.001, Student's *t* test).
(F) ABA-inhibited stomatal opening in the wild type, *ear1-1*, *OE-16#*, and *OE-28#*. Four-week-old plants were grown in a dark room for 24 h to close their stomata, and epidermal strips from the plants were treated with or without 10 μM ABA in the light for 2 h before being photographed. Bars are means ± SE of three biological replicates (20 stomata from one seedling per replicate). The asterisks indicate significant differences compared with the wild type treated with ABA (***P < 0.001, Student's *t* test).
(G) and **(H)** Leaf temperature in the wild type, *ear1-1*, *OE-16#*, and *OE-28#*. Four-week-old plants were used for thermal imaging measurements **(G)**. Bars in **(H)** are means ± SE of three replicates (15 leaves from one pot were measured per replicate, and three different pots were analyzed). The asterisks indicate significant differences compared with the wild type treated with ABA (***P < 0.001, Student's *t* test).
(I) Water loss in detached leaves from the wild type, *ear1-1*, *OE-16#*, and *OE-28#*. Four-week-old plants were used for relative water loss measurements. Data are means ± SE of three biological replicates (~40 leaves were measured per replicate) from one experiment. Three independent experiments were performed, with similar results.
(J) Transpiration rates in the wild type, *ear1-1*, *OE-16#*, and *OE-28#*. Four-week-old seedlings were used for the transpiration assay. Bars are means ± SE of plants in three different pots.
(K) Drought phenotypes in the wild type, *ear1-1*, *OE-16#*, and *OE-28#* in soil. Three-week-old seedlings were subjected to drought stress; watering was withheld for 7 d (top panel) and 12 d (bottom panel) before the plants were photographed.

Downloaded from https://academic.oup.com/plcell/article/30/4/815/6099023 by guest on 21 August 2022

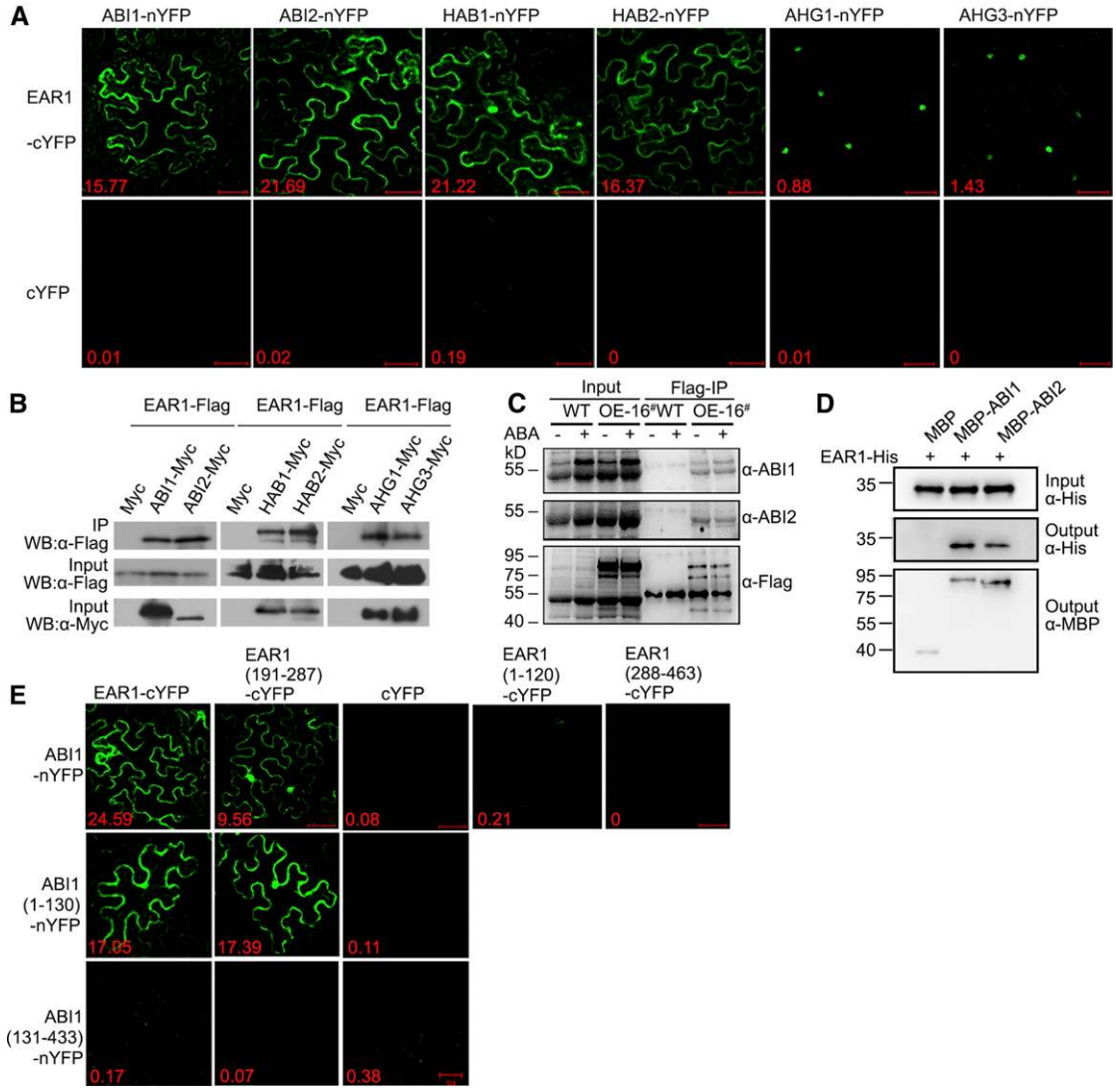

Figure 5. EAR1 Physically Interacts with Clade A PP2Cs.

(A) EAR1 interacts with six PP2Cs in *N. benthamiana* leaves in a BiFC assay. The EAR1 coding sequence (CDS) was fused to the C terminus of YFP, and the CDS of each PP2C was fused with the N terminus of YFP. The constructs were coinjected into *N. benthamiana* leaves, and YFP signals were observed after 48 to 72 h. Quantification of YFP signals was performed with ImageJ software; the values represent the YFP fluorescence intensity in 0.04 mm^2 (the whole field) and are shown at the bottom. Bars = 50 μm.

(B) EAR1 is coimmunoprecipitated with all six PP2Cs in Arabidopsis protoplasts. *Pro35S:EAR1-Flag* was cotransformed into Arabidopsis mesophyll protoplasts with *Pro35S:ABI1-Myc*, *Pro35S:ABI2-Myc*, *Pro35S:HAB1-Myc*, *Pro35S:HAB2-Myc*, *Pro35S:AHG1-Myc*, *Pro35S:AHG3-Myc*, and *Pro35S:Myc*. After 14 to 16 h of incubation, total proteins were used for immunoprecipitation (IP) with anti-Myc agarose, and the eluted fractions were detected by immunoblot analysis (protein gel blot [WB]) with anti-Flag antibodies. Total proteins (Input) were detected with anti-Flag and anti-Myc antibodies.

(C) Co-IP assay showing the interaction of ABI1 or ABI2 with EAR1-Flag in Arabidopsis seedlings. Total proteins from a wild-type plant or the homozygous transgenic plant *OE-16#* (Input) treated with or without ABA were immunoprecipitated with anti-Flag M2 affinity gel (Flag-IP), and ABI1 or ABI2 was detected with anti-ABI1 or anti-ABI2 antibody, respectively. EAR1-Flag was detected with anti-Flag antibody.

(D) ABI1/ABI2 can pull down EAR1. MBP-ABI1, MBP-ABI2, MBP, and EAR1-His proteins were expressed in *E. coli*. Purified proteins were used for the pull-down assay. MBP-ABI1, MBP-ABI2, and MBP were detected with anti-MBP antibodies, and EAR1-His proteins were detected with anti-His antibodies.

(E) $EAR1^{191-287}$ interacts with the N terminus of ABI1 in *N. benthamiana* leaves, as revealed by BiFC. Different truncations of EAR1 and ABI1 were fused with the C terminus of YFP and the N terminus of YFP, respectively. The constructs were coinjected into *N. benthamiana* leaves, and YFP signals were observed after 48 to 72 h. The quantification of YFP signals is shown at the bottom of each panel. Bars = 50 μm.

Downloaded from https://academic.oup.com/plcell/article/30/4/815/6099023 by guest on 21 August 2022

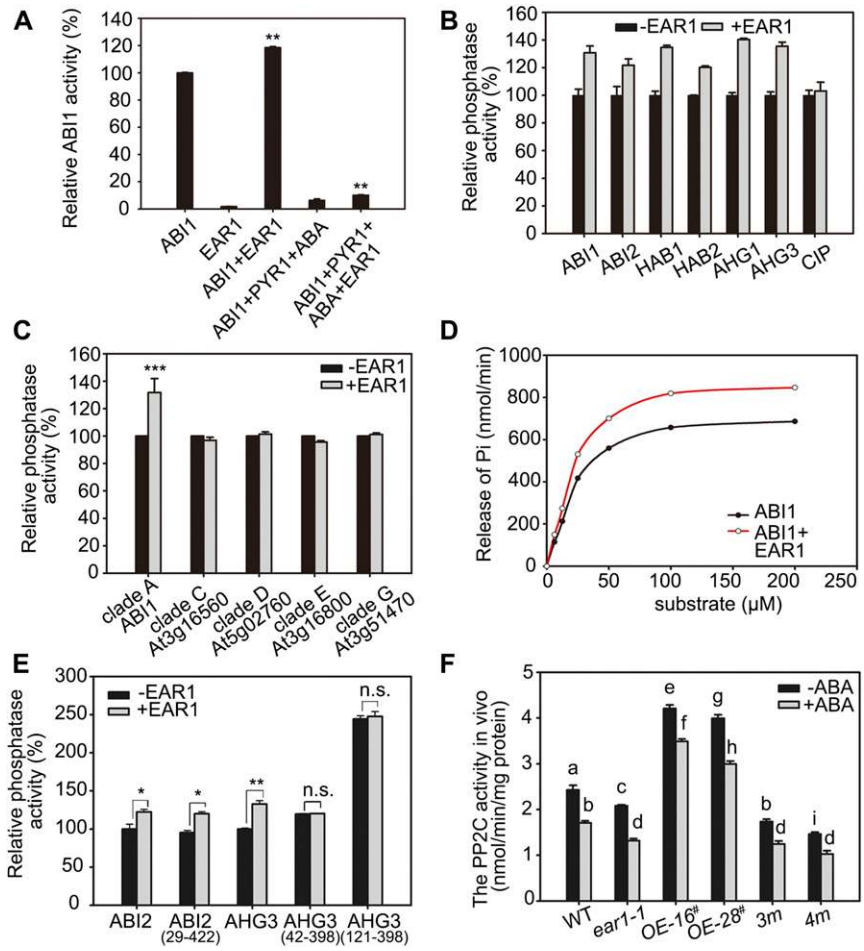

Figure 6. EAR1 Enhances the Activity of Clade A PP2Cs.

(A) EAR1 enhances the phosphatase activity of ABI1 in vitro. Recombinant ABI1 and EAR1$^{121-287}$ proteins were used for the phosphatase activity assay; the concentrations of ABI1 and EAR1 were 0.5 and 4 μM, respectively. The phosphatase activity of ABI1 was set to 100%. The combination of ABI1 and PYR1 with ABA was also included for comparison. The concentrations of PYR1 and ABA were 2 and 5 μM, respectively. Bars are means ± SE of three biological replicates (**P < 0.01, Student's *t* test). Each replicate was independently measured at different times.

(B) EAR1 enhances the phosphatase activities of six PP2Cs in vitro. Phosphatase activity was measured using various combinations of EAR1$^{121-287}$ with different PP2C proteins. The phosphatase activity of each PP2C was set to 100%. Calf intestinal alkaline phosphatase (CIP) was used as a negative control. Bars are means ± SE of three biological replicates. Each replicate was independently measured at different times.

(C) EAR1 does not enhance the phosphatase activities of other PP2Cs. Different combinations of EAR1$^{121-287}$ peptide and a representative member of each of the five clades of PP2C proteins (clade A, *ABI1*; clade C, *At3g16560*; clade D, *At5g02760*; clade E, *At3g16800*; and clade G, *At3g51470*) were mixed for the phosphatase activity assay. The phosphatase activity of each clade PP2C was set to 100%. Bars are means ± SE of three biological replicates (***P < 0.001, Student's *t* test). Each replicate was independently measured at different times.

(D) Kinetic-dependent curve of ABI1 phosphatase activity with or without EAR1. Recombinant proteins of ABI1 and EAR1$^{121-287}$ were used for the phosphatase activity assay. The substrate concentrations were 100, 50, 25, 12.5, and 6.25 μM, and ABI1 phosphatase activity was measured using each concentration of substrate. The concentrations of ABI1 and EAR1 were 0.5 and 4 μM, respectively. The calculated K_m of ABI1 with or without EAR1 was 18.6 or 20.8 μM, respectively; the K_{cat} of ABI1 with or without EAR1 was 240.5 or 203.3 s^{-1}, respectively; and the V_{max} of ABI1 with or without EAR1 was 909.1 or 769.2 nmol/min, respectively. The experiments were performed three times with similar results, and the Michaelis parameters were calculated based on three measurements.

(E) Phosphatase activity of truncated ABI2 and AHG3. Equal amounts of ABI2 and ABI2$^{29-422}$ or AHG3, AHG3$^{42-398}$, and AHG3$^{121-398}$ were mixed with or without EAR1 for the phosphatase activity assays. The phosphatase activity of ABI2 and AHG3 without EAR1 was set to 100%. Bars are means ± SE of three biological replicates (n.s., no significant difference; *P < 0.05 and **P < 0.01, Student's *t* test). Each replicate was independently measured at different times.

(F) Total PP2C activity in *ear1-1*, the wild type, overexpression lines *OE-16#* and *OE-28#*, and the *3m* and *4m* mutants. Total proteins were extracted from 10-d-old seedlings treated with or without 60 μM ABA for 1 h. PP2C activity was measured after the addition of 5 μM okadaic acid to inhibit the activity of PPP family Ser/Thr-specific phosphoprotein phosphatases (e.g., PP1 and PP2A). Bars are means ± SE of three biological replicates (different letters represent significant differences at P < 0.01, Student's *t* test). Each replicate was independently measured with differently treated samples. PP2C activity is represented as the amount of phosphate dephosphorylated by PP2C released per minute.

Downloaded from https://academic.oup.com/plcell/article/30/4/815/6099023 by guest on 21 August 2022

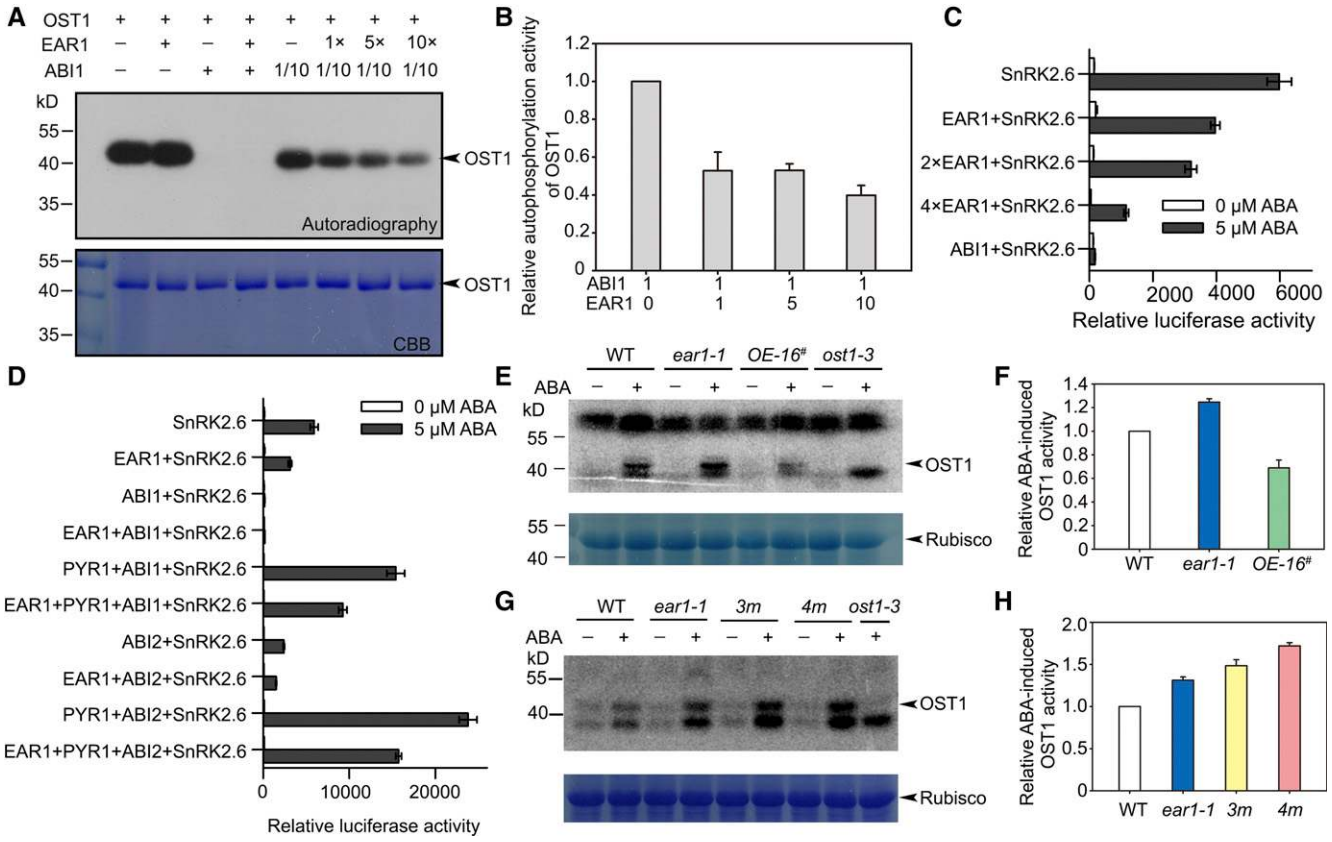

Figure 7. EAR1 Represses ABA Signaling.

(A) EAR1 reduces OST1 activity by enhancing the phosphatase activity of ABI1 in vitro. Recombinant proteins with OST1 (4 μg), ABI1 (100 ng is indicated as + and 10 ng as 1/10), and EAR1 (from 4 to 40 ng) were combined for the kinase assay. OST1 was used as a substrate and stained with Coomassie Brilliant Blue (CBB) as a loading control. The experiments were performed three times, with similar results.

(B) Quantitative analysis of the OST1 band intensity in **(A)** with ImageJ software. The OST1 band intensity of ABI1 without EAR1 was set to 1 as a reference compared with the OST1 band intensities of ABI1 with 1×, 5×, or 10× EAR1. Bars are means ± SE from three independent experiments.

(C) EAR1 inhibits the expression of ABA-responsive genes in a reconstitution assay of the ABA signaling pathway. *ProRD29B:LUC* was cotransformed with *Pro35S:EAR1*, *Pro35S:ABI1*, and *Pro35S:SnRK2.6* into *snrk2.2/snrk2.3/snrk2.6* (*snrk2.2/2.3/2.6*) triple mutant protoplasts treated with or without ABA. Luciferase activity was used as an indicator of the expression of the ABA-responsive gene *RD29B*, and *ZmUBQ:GUS* was used as an internal control. Bars are means ± SE of three biological replicates. Each replicate was independently measured at different times.

(D) EAR1 suppresses the core ABA signaling genes in a reconstitution assay of the ABA signaling pathway. *ProRD29B:LUC* was coexpressed with *Pro35S:EAR1*, *Pro35S:ABI1*, *Pro35S:ABI2*, *Pro35S:PYR1*, and *Pro35S:SnRK2.6* in *snrk2.2/snrk2.3/snrk2.6* (*snrk2.2/2.3/2.6*) triple mutant protoplasts treated with or without ABA. Luciferase activity was used as an indicator of the expression of the ABA-responsive gene *RD29B*, and *ZmUBQ:GUS* was used as an internal control. Bars are means ± SE of three biological replicates. Each replicate was independently measured at different times.

(E) OST1 kinase activity is enhanced in *ear1-1* and reduced in the EAR1 overexpression line *OE-16#* in an in-gel kinase assay. Total proteins (80 μg) were extracted from 10-d-old wild-type, *ear1-1*, *OE-16#*, and *ost1-3* seedlings treated with or without 60 μM ABA for 30 min. The proteins were separated on a 10% SDS-PAGE gel with GST-ΔABF2 as a substrate. Rubisco was used as a loading control. The experiments were performed three times, with similar results.

(F) Quantitative analysis of the band intensity in **(E)**. The band intensity in the wild type was set to 1 as a reference, and the band intensity of *ear1-1* or *OE-16#* was compared with that of the wild type. Bars are means ± SE from three independent experiments.

(G) OST1 kinase activity is enhanced in *ear1-1*, *3m*, and *4m*. Total proteins (80 μg) were extracted from 10-d-old seedlings treated with or without 30 μM ABA for 30 min. The proteins were separated on a 10% SDS-PAGE gel with GST-ΔABF2 as a substrate. Rubisco was used as a loading control. The experiments were performed three times, with similar results.

(H) Quantitative analysis of the band intensity in **(G)**. The band intensity in the wild type was set to 1 as a reference. Bars are means ± SE (n = 3 three independent experiments).

its activity was not further enhanced by EAR1, although its activity was higher than that of the full-length protein (Figure 6E). When we removed 120 amino acids from the N terminus of AHG3, its activity further increased, which was not enhanced by EAR1 (Figure 6E). These results suggest that the N termini of these PP2Cs function as inhibition domains and that EAR1 plays a crucial role in releasing the inhibition of the N termini of PP2Cs at their catalytic domains.

We then compared PP2C activity among the wild-type, *ear1-1*, *OE-16#*, *OE-28#*, *3m*, and *4m* genotypes using okadaic acid, which

Downloaded from https://academic.oup.com/plcell/article/30/4/815/6099023 by guest on 21 August 2022

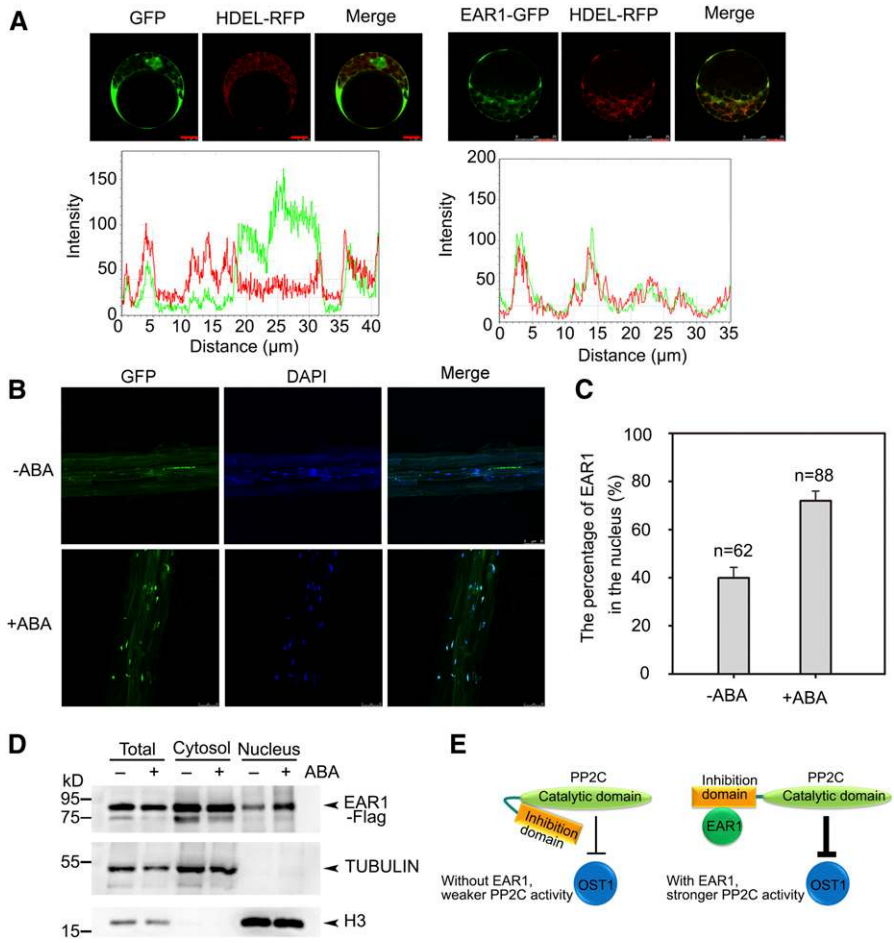

Figure 8. ABA Promotes the Translocation of EAR1 from the ER or Cytosol to the Nucleus.

(A) The location of EAR1 in Arabidopsis protoplasts. *ProSuper:GFP* (GFP) or *ProSuper:EAR1-GFP* (EAR1-GFP) was coexpressed in Arabidopsis leaf protoplasts with *Pro35S:HDEL-RFP* (HDEL-RFP). GFP and RFP signals were analyzed. The green curve represents GFP signals, and the red curve represents RFP signals. Bars = 10 μm.

(B) ABA promotes the translocation of EAR1 from the ER and/or cytosol to the nucleus. Seven-day-old *COM-22* transgenic plants (*ProEAR1:EAR1-GFP*) were treated with or without 60 μM ABA for 1 h, and GFP signals were observed under a confocal laser-scanning microscope. 4′,6-Diamidino-2-phenylindole (DAPI) staining shows the locations of nuclei. Bars = 50 μm.

(C) Statistical analysis of the percentage of EAR1 in the nucleus with or without ABA treatment. Seven-day-old *COM-22* transgenic plants (*ProEAR1:EAR1-GFP* complemented *ear1-1*) were treated with or without 60 μM ABA for 1 h, and the total numbers of nuclei and nuclei containing GFP were analyzed. A total of 62 and 88 nuclei without and with ABA treatment, respectively, were used for analysis. Without ABA treatment, very weak GFP signals were detected in the nuclei. Bars are means ± SE of three biological replicates. Approximately 20 cells from different seedlings were analyzed in each replicate.

(D) ABA promotes the accumulation of EAR1 in the nucleus. Total proteins were extracted from 2-week-old *OE-16*$^{\#}$ transgenic plants treated with or without 60 μM ABA, and the cytoplasmic and nuclear fractions were separated. The proteins were then detected by immunoblotting analysis. TUBULIN was used as a cytoplasmic fraction marker, and H3 protein served as a nuclear fraction marker.

(E) A proposed model for the role of EAR1 in the ABA signaling pathway. In the absence of EAR1, the N-terminal autoinhibition domain of PP2C inhibits its activity. When EAR1 interacts with the N terminus of PP2C, it releases the autoinhibition of PP2C and increases its activity.

is ineffective toward PP2C but can inhibit the activity of PPP family proteins (e.g., PP1 and PP2A) (Zhao et al., 2017) (Figure 6F). Ten-day-old seedlings were treated with 60 μM ABA for 1 h, and total proteins were extracted and used for the PP2C assay. Consistent with the ABA-sensitive phenotypes, *OE-16*$^{\#}$ showed the highest PP2C activity and *4m* the lowest, both with and without ABA treatment. The PP2C activity of *ear1-1* was higher than that of *3m* and *4m* and lower than that of *OE-28*$^{\#}$ and the wild type. Our comparisons of the wild type with *ear1-1* and of the triple mutant with the quadruple mutant revealed that EAR1 enhances PP2C activity in plants.

We also analyzed whether EAR1$^{121-287}$ could attenuate OST1 activity by enhancing ABI1 activity using proteins isolated from *E. coli*. As shown in Figures 7A and 7B, OST1 itself (4 μg) displayed autophosphorylation activity (Figure 7A, first lane), and the addition of EAR1$^{121-287}$ (0.004 μg) did not affect OST1 activity

Downloaded from https://academic.oup.com/plcell/article/30/4/815/6099023 by guest on 21 August 2022

(Figure 7A, second lane). When OST1 was incubated with 0.1 μg of ABI1, its autophosphorylation activity was completely inhibited (Figure 7A, third lane). When 0.004 μg of EAR1 was added to the reaction mixture, the autophosphorylation activity of OST1 was still completely inhibited by ABI1 (Figure 7A, fourth lane). We then diluted the ABI1 10-fold and added it to the reaction mixture. At this ABI1 concentration (0.01 μg; Figure 7A, fifth lane), we detected OST1 autophosphorylation activity, indicating that this concentration of ABI1 is not sufficient to completely inhibit OST1 activity. At this ABI1 concentration, OST1 autophosphorylation activity gradually decreased with increasing amounts of $EAR1^{121-287}$ protein (from 0.004 [sixth lane] to 0.04 μg [eighth lane]; Figures 7A and 7B). These results suggest that EAR1 does not affect OST1 activity directly but instead enhances ABI1 activity to inhibit the activity of OST1.

We then used transient activation assays to determine whether EAR1 affects the phosphorylation activity of SnRK2.6/OST1 in cells. When SnRK2.6/OST1 was transiently expressed in protoplasts from the *snrk2.2/snrk2.3/snrk2.6* triple mutant, OST1 phosphorylated and activated ABF2 only in the presence of ABA. Activated ABF2 induces the expression of *RD29B-LUC* (Fujii et al., 2009). As shown in Figure 7C, the luciferase activity of *RD29B-LUC* gradually decreased when OST1 was coexpressed with increasing amounts of EAR1 in the presence of ABA. In this assay, ABA treatment induced the transcription of *ABI1* and *ABI2*, as demonstrated previously (Kong et al., 2015). The addition of ABI1 or ABI1 plus EAR1 completely inhibited the activity of OST1, as determined based on *RD29B-LUC* activity (Figure 7D). The addition of PYR1 and ABA together with ABI1 and SnRK2.6/OST1 recovered OST1 activity, whereas OST1 activity was reduced by the addition of EAR1. Similar results were obtained when ABI1 was exchanged with ABI2 in the above assays.

The effects of altered activity of clade A PP2Cs on ABA signaling can be determined based on the strength of ABA-activated OST1 activity. Therefore, we measured OST1 activity using ABF2 (amino acids 73 to 118) as an OST1-specific substrate in in-gel assays. The *ost1-3* mutant was used as a negative control, as it does not exhibit OST1 activity. The *ear1-1* mutant exhibited slightly higher OST1 activity than the wild type, whereas the EAR1-overexpressing transgenic line *OE-16#* had the lowest OST1 activity compared with *ear1-1* and the wild type (Figures 7E and 7F). Although the *ear1-1/abi1-2/abi2-2/hab1-1* quadruple mutant exhibited higher OST1 activity than the *abi1-2/abi2-2/hab1-1* triple mutant after ABA treatment, OST1 was not constitutively activated in the *4m* mutant in the absence of ABA treatment (Figures 7G and 7H). This result is consistent with the previous finding that OST1 is not constitutively activated in the *abi1-2/abi2-2/hab1-1/pp2ca-1* quadruple mutant (Brandt et al., 2015). These results suggest that EAR1 decreases OST1 activity by enhancing PP2C activity both in vivo and in vitro.

Next, we examined whether the expression of genes regulated by the ABA signaling pathway was altered in *ear1-1* and the *EAR1* overexpression lines. We selected several marker genes that are positively regulated by ABA signaling and measured their expression via RT-qPCR. The expression levels of all these genes, including *RD29A* (*Responsive to desiccation29A*), *RD29B*, *RAB18* (*Responsive to ABA18*), *ABF4* (*ABRE binding factor4*), *P5CS1* (*Delta 1-pyrroline-5-carboxylate synthase1*), and *KIN1* (*Kinase1*), were higher in *ear1-1* and the *abi1-2/abi2-2/hab1-1* triple loss-of-function mutant and lower in *EAR1 OE-16#* than in the wild type (Supplemental Figure 8). These results indicate that EAR1 plays a negative role in regulating the expression of genes involved in ABA signaling.

ABA Promotes the Translocation of EAR1 from the Endoplasmic Reticulum or Cytoplasm to the Nucleus

To investigate the localization of EAR1, we transiently expressed a *Super* promoter driving *EAR1-GFP* in Arabidopsis protoplasts and in *N. benthamiana* leaves via Agrobacterium infiltration. The endoplasmic reticulum (ER) marker protein HDEL-RFP was used as a control in this experiment. EAR1-GFP mainly colocalized with HDEL-RFP (Figure 8A; Supplemental Figure 9A). In transgenic plants expressing *ProEAR1:EAR1-GFP*, GFP signals were also weakly detected in nuclei and possibly also in the cytoplasm (Figure 8B). Interestingly, EAR1-GFP accumulated to higher levels in nuclei after 30 min of ABA treatment (Figures 8B and 8C). Immunoblotting using proteins extracted from transgenic plants expressing *Pro35S:EAR1-Flag* indicated that EAR1 was detected in both the cytosol and the nuclear fraction in the absence of ABA treatment, whereas ABA treatment significantly increased the accumulation of EAR1 in nuclei (Figure 8D). When we separated the proteins into the microsomal and the soluble fractions, EAR1 was detected in both fractions (Supplemental Figure 9B). These results indicate that ABA signaling promotes the translocation of EAR1 from the ER and/or cytoplasm to the nucleus.

According to the above study, we proposed a model to explain the biological roles of EAR1 in enhancing PP2C activity (Figure 8E).

DISCUSSION

The protein Ser/Thr-specific phosphatases (PSPs) play crucial roles in dephosphorylating thousands of phosphoproteins. Compared with protein Ser/Thr kinases (PSKs), there are fewer PSPs: the human genome encodes 428 PSKs versus 31 PSPs, whereas in Arabidopsis, there are ~1000 PSKs but only 102 PSPs (Kerk et al., 2008; Shi, 2009). How these PSPs are dynamically regulated by different proteins or compounds has attracted increasing attention in recent years. Most members of the PPP family have both catalytic subunits and various regulatory subunits (Shi, 2009). In contrast to the PPP subfamily, members of the PPM subfamily generally do not contain regulatory subunits, but they exhibit other conserved domains or motifs that determine substrate specificity (Shi, 2009). However, PP5 in the PPP subfamily is unique because it comprises only one polypeptide that contains both catalytic and regulatory domains. The N terminus of PP5 contains a tetratricopeptide repeat (TPR) regulatory domain that engages with the catalytic domain, thus inhibiting phosphatase activity by restricting substrate access to the catalytic site (Yang et al., 2005). Hsp90 and fatty acids interact with the TPR domain, disrupt the TPR-phosphatase domain interaction, and activate its phosphatase activity (Yang et al., 2005). Clade A PP2Cs involved in ABA signaling have short, nonconserved N-terminal regulatory domains and conserved C-terminal catalytic domains that interact with and are inhibited by ABA-bound PYR1/PYL/RCARs (Melcher et al., 2009; Miyazono et al., 2009;

Downloaded from https://academic.oup.com/plcell/article/30/4/815/6099023 by guest on 21 August 2022

Park et al., 2009; Santiago et al., 2009; Yin et al., 2009; Hao et al., 2011). It has long been known that the N-terminal domain plays an autoinhibitory role in regulating ABI1 activity (Sheen, 1998). However, whether this inhibition domain is regulated by other proteins is currently unknown. Our genetic and other analyses indicated that EAR1 negatively regulates ABA signaling by increasing PP2C activity and reducing OST1 activity and negatively regulates the expression of genes involved in ABA signaling (Figure 8F).

Previous studies have suggested that ROP11 GTPase interacts with ABI1 or ABI2, which likely protects ABI1/ABI2 phosphatase activity from inhibition by PYLs (Yu et al., 2012). Our data indicate that EAR1 interacts with all six ABA-related PP2Cs, releasing their autoinhibition of the N termini and increasing PP2C activity in vitro. We found that the presence of increasing levels of EAR1 protein gradually reduced OST1 activity when ABI1 protein levels were unchanged in an in vitro assay (Figures 6A and 6B). In a transient expression cell assay, increasing the expression of EAR1 also decreased OST1 activity (Figures 6C and 6D). The EAR1-induced increase in PP2C activity was also reflected by the OST1 activity measured in an in-gel assay in the wild type, *ear1-1* mutant, *EAR1*-overexpressing lines, *abi1-2/abi2-2/hab1-1/pp2ca-1*, and *ear1-1/abi1-2/abi2-2/hab1-1* (Figures 7E to 7H). Under normal conditions, OST1 is not activated, even in *abi1-2/abi2-2/hab1-1/pp2ca-1* (Brandt et al., 2015) and *ear1-1/abi1-2/abi2-2/hab1-1* quadruple mutants. The expression of *EAR1* and its protein levels were not altered by ABA treatment (Figure 7E), but ABA treatment led to the accumulation of EAR1 in the nucleus (Figure 7). Given that ABA treatment induces the expression of *PP2Cs* (Kong et al., 2015), that PYR1/PYLs in turn inhibit PP2C activity in the presence of ABA, and that PP2Cs and PYLs are dynamically regulated by the 26S proteasome (Bueso et al., 2014; Irigoyen et al., 2014; Li et al., 2016), the complexity of this ABA signaling pathway makes it difficult to determine exactly how EAR1 affects PP2C activity during ABA treatment in vivo. In the in vivo assays, we mainly detected changes in total PP2C activity in the presence or absence of EAR1. As EAR1 interacts with the N terminus of each PP2C, which does not interfere with the interaction between PP2Cs and PYLs, it is possible that EAR1 quickly enhances PP2C activity when the inhibition of PP2Cs is released from PYLs during recovery from drought stress. The changes in the location of EAR1 might also affect the activity of PP2Cs in different sites of the cell under ABA treatment. Perhaps EAR1 increases the activity of ABI1 (or other PP2Cs) not only under normal conditions (to effectively repress ABA signaling) but also under drought stress; this process would dynamically regulate the homeostasis of ABA signaling to allow the plant to quickly respond to drought stress. Similarly, the degradation of ABI1 only occurs when ABI1 interacts with PYR1/PYLs in either the presence or absence of ABA (Kong et al., 2015). Thus, in this study, we identified a previously uncharacterized mechanism for the positive regulation of clade A PP2Cs by EAR1 during ABA signaling.

Notably, EAR1 interacted with six clade A PP2Cs involved in ABA signaling but not with the other types of PP2Cs examined. However, the clade A-type PP2Cs possess different, non-conserved N termini. How EAR1 selectively recognizes these different N termini is still unknown. One promising explanation is that perhaps EAR1 is an IDR that interacts with the disordered N terminus of a PP2C, forming a relatively stable structure. IDPs with short interaction-prone segments are characterized by promiscuity and plasticity and are more likely to bind to multiple partner proteins (Sun et al., 2013). Once IDPs interact with other proteins, their structures change from disordered to ordered, and they form a relatively stable complex. This fold-upon binding feature may rely on the short MoRFs localized in the IDRs (Sun et al., 2013). Recent studies have described several well-characterized plant IDPs, including GRAS (for GIBBERELLIC ACID INSENSITIVE, REPRESSOR OF GAI, and the SCARECROW) proteins, LEA (LATE EMBRYOGENESIS ABUNDANT) proteins, NAC and bZIP transcription factors, and CRY family proteins (Sun et al., 2013). The present results indicate that EAR1 can interact with the N termini of all six clade A PP2Cs, possibly resulting in the formation of a stable, ordered structure, thereby relieving the autoinhibition of the N-terminal domain. Interestingly, in AHG3, the 42-amino acid fragment at the N terminus contains one putative MoRF that determines its interaction with EAR1, and its activity is enhanced by EAR1. However, the N terminus of AHG3 lacking the first 42 amino acids can still exert its inhibitory effect on the catalytic domain of this protein, and the removal of these amino acids did not affect EAR1-enhanced ABI2 activity. EAR1 has two relatively conserved domains: one around 133 to 167 and another one around 224 to 278 (Supplemental Figure 2B). The latter domain is required for its interaction with the N termini of PP2Cs (Figure 5E; Supplemental Figure 4C), while the former domain should contain an important functional feature. As shown in Figure 2D, the fragment 141 to 190 is required for the full roles of EAR1 in the ABA response. These results suggest that both domains play different crucial roles in EAR1. Further studies involving the analysis of the interaction of EAR1 with PP2Cs by examining their crystal structures are needed to explore their molecular connection in more detail.

METHODS

Plant Materials and Growth Conditions

In this study, *Arabidopsis thaliana* plants harboring a *gl1* mutation in the Col-0 background were used as the wild type. The seeds were sown on MS medium containing 2% (w/v) sucrose and 0.8% or 1% (w/v) agar, incubated at 4°C for 3 d, and transferred to a light incubator (Philips F17T8/TL841 bulb) under a 22-h-light/2-h-dark cycle with a light intensity of 60 μE m^{-2} s^{-1} at 22°C. For the root-bending assays, 4-d-old seedlings were transferred to MS medium containing different concentrations of ABA and grown for an additional 7 d. For the germination assays, ~30 seeds were sown on MS medium containing different concentrations of ABA. The plates were transferred from a temperature of 4°C to the light incubator, where they were grown for 7 d to examine the seed germination ratio, with three plates prepared per experiment. For physiological experiments, the seedlings were grown in pots containing a mixture of forest soil:vermiculite (1:1) under a 12-h-light/12-h-dark cycle in a greenhouse for 3 or 4 weeks.

A T-DNA line, SALK_057606 (*ear1-2*), with T-DNA inserted at 1088 bp of the *AT5G22090* gene, was obtained from the Arabidopsis Biological Resource Center. A homozygous T-DNA insertion line was obtained using PCR. The ABA phenotypes of *ear1-2* (the progeny of a cross between *ear1-1* and *ear1-2*) were analyzed.

The other mutants used in this study included *abi1-2* (SALK_072009), *abi2-2* (SALK_015166), *hab1-1* (SALK_002104), *ost1/snrk2.6* (SALK_008068), *snrk2.2* (GABI-Kat 807G04), and *snrk2.3* (SALK_107315). The *pp2c* triple mutant (*3m*) was established by crossing *abi1-2*, *abi2-2*, and *hab1-1*, and the *4m* mutant was

Downloaded from https://academic.oup.com/plcell/article/30/4/815/6099023 by guest on 21 August 2022

established by crossing *3m* and *ear1-1*. The primers used to examine these mutants are listed in Supplemental Data Set 4.

Map-Based Cloning and Mutant Complementation

The *ear1-1* mutant was crossed with Landsberg *erecta* to obtain the F2 population for selection of mutant plants based on increased ABA sensitivity in roots on MS medium containing 30 μM ABA. Approximately 2819 *ear1-1* seedlings were chosen to map *EAR1* using SSLP markers. *EAR1* was initially mapped to chromosome 5 between BAC clones F8L15 and MOP9, and the locus was then narrowed down to T10F18 and MWD9 using the markers MPI7, F5O24, F22D1, T10F18, T6G21, and MWD9. All genes in this region were sequenced, and only one mutation, C163 to T163, was identified in *AT5G22090*, which caused a premature stop codon.

To complement the *ear1-1* mutant, the complete *EAR1* sequence was amplified by PCR using genomic DNA as a template. The resulting DNA fragment was ligated into the pCAMBIA1391 vector at the *Pst*I and *Bgl*II restriction enzyme sites. The resulting construct was transformed into *Agrobacterium tumefaciens* GV3101 and transferred to *ear1-1* plants using the floral dip method (Clough and Bent, 1998). The transgenic plants were screened on MS medium containing 30 mg/L hygromycin to obtain homozygous lines for examining ABA phenotypes.

To produce the various truncations to complement the *ear1-1* phenotype, the *EAR1* promoter was cloned into pCAMBIA1391 between the *Pst*I and *Eco*RI sites, and the truncated CDS fragments were cloned into the vector at the *Nco*I and *Pml*I sites. The constructs were subsequently transformed into Agrobacterium GV3101 and transferred into *ear1-1* plants as described above.

Subcellular Localization and GUS Staining

The *EAR1* cDNA PCR products were cloned into the *Xba*I and *Spe*I sites of a modified vector, pCAMBIA 1300, which contains a superpromoter before the *Xba*I site and GFP cDNA after the *Spe*I site. This construct was then transformed into Agrobacterium GV3101 and injected into *Nicotiana benthamiana* leaves using an HDEL tag (Liu et al., 2011) as an ER marker. The plants were subsequently grown at 18°C under a 12-h-light/12-h-dark cycle in a greenhouse for 48 to 72 h prior to observation. The GFP and RFP signals were detected under a Zeiss LSM 510 META confocal laser-scanning microscope. The GFP images were acquired at excitation of 488 nm and emission of 525 nm, and the RFP images were acquired at excitation of 543 nm and emission at 615 nm.

To determine the subcellular localization of EAR1 in the transgenic plants, full-length *EAR1* cDNA was fused with *GFP* in-frame and cloned into pCAMBIA1391 under the control of the *EAR1* native promoter, and the correct construct was transformed into Agrobacterium GV3101. The Agrobacterium was transferred into *ear1-1* plants via the floral dip method, and T3 homozygous transgenic seedlings (numbers 6 and 22) that complemented the ABA-sensitive phenotypes of *ear1-1* were used for GFP analysis.

For GUS staining, the *EAR1* promoter was cloned into pCAMBIA1391 between the *Pst*I and *Eco*RI sites. The construct was subsequently transformed into Agrobacterium GV3101 and transferred into plants using the floral dip method. T3 hygromycin-resistant transgenic seedlings were used for the GUS staining assay.

Physiological Experiments

All physiological experiments were performed as described previously with some modifications (He et al., 2012). To assay water loss in detached leaves, shoots were cut from plants that had been grown for 4 weeks under normal conditions. The shoots were placed on a piece of weighing paper under a light in the greenhouse, weighed immediately after excision, and periodically weighed every hour. The results are shown as a percentage of the fresh weight. More than two independent experiments were performed, each including three or four replicate shoots per line.

For the stomatal aperture assay, epidermal strips were peeled from 4-week-old plants, and the mesophyll cells were removed with a small brush. To examine ABA-mediated stomatal closure, the epidermal strips were incubated in MES buffer (10 mM MES-KOH, pH 6.15, 10 mM KCl, and 50 μM $CaCl_2$) in the light for 2 h at 22°C to open the stomata. After the addition of 20 μM ABA to the buffer and incubation of the epidermal strips for an additional 2 h in the light at 22°C, images were obtained under a microscope (Olympus BX53). To examine the ABA-mediated inhibition of stomatal opening in the light, 4-week-old plants were incubated in a dark room for 24 h to close the stomata. Epidermal strips from the plants were then incubated in MES buffer with or without ABA in the light at 22°C for 2 h, after which the epidermal strips were photographed under a microscope (Olympus BX53). The stomata in the images were measured using ImageJ software.

To assess drought-stress tolerance, 7-d-old seedlings were transferred to pots, grown for 2 weeks under normal conditions, and subjected to drought conditions by withholding water from the seedlings for 2 weeks. The drought phenotypes were photographed with a camera (Nikon D80).

Gas-Exchange Measurement

Gas exchange in leaves was measured as described previously (Chen et al., 2011). In brief, the plants were grown at 18°C under a 12-h-light/12-h-dark cycle in a greenhouse for 3 weeks. Water was withheld for 1 week before measurement. The transpiration rate and the photosynthetic rate were determined using an LI-6400XT infrared gas analyzer (LI-COR) at a PAR level of 1000 μmol m^{-2} s^{-1}. Each plant in a pot was placed into a leaf chamber, and the transpiration rate and photosynthetic rate were measured after 5 min. For each genotype, plants in three different pots were examined, with similar results.

Thermal Imaging

Thermal imaging of plants was performed as described previously with some modifications (Hua et al., 2012). Briefly, the plants were grown at 18 to 20°C under a 12-h-light/12-h-dark cycle in a greenhouse for 3 weeks. Water was then withheld for 1 week before measurements. Thermal images were obtained using a VarioCAM HD infrared camera (JENOPTIK). Leaf temperature was measured using IRBIS 3 professional software. For each genotype, plants in three different pots were analyzed, with similar results.

Phylogenetic Analysis

The amino acid sequences of EAR1 in each species were acquired from the BLAST tool in the National Center for Biotechnology Information database (http://blast.ncbi.nlm.nih.gov/Blast.cgi). Multiple alignments of amino acid sequences were aligned using ClustalX. Phylogenetic analysis was performed with the MEGA4.0 program by the neighbor-joining method with 1000 bootstrap sampling using full-length sequences.

Quantitative RT-PCR

Total RNA was extracted from 7-d-old seedlings with TRIzol reagent (Life Technologies). The RNA was reverse transcribed to cDNA with MMLV reverse transcriptase (Promega). Quantitative RT-PCR was performed on a 7300 Real-Time PCR system (Applied Biosystems) using SYBR Premix Ex Taq (TaKaRa). *UBQ* was used as an internal control. For each genotype, three different samples were used as three replicates.

Protein Purification

Proteins with different tags were expressed in BL21 *Escherichia coli* cells with 0.5 mM IPTG for 18 h at 20°C. The culture was then collected by centrifugation at 6000*g* for 10 min at 4°C.

Downloaded from https://academic.oup.com/plcell/article/30/4/815/6099023 by guest on 21 August 2022

For His-tagged proteins, the pellet was resuspended in lysis buffer (50 mM NaH_2PO_4, 30 mM NaCl, 10 mM imidazole, pH 8.0, 1 mM PMSF, and 1× cocktail) and sonicated for 10 min. After centrifugation for 30 min at 7000*g*, the supernatant was incubated with Ni Sepharose (GE) resin for 3 h at 4°C. The resin was washed three times with washing buffer (50 mM NaH_2PO_4, 30 mM NaCl, and 50 mM imidazole, pH 8.0) to remove nonspecifically bound proteins. The His-tagged proteins were eluted from the resin with elution buffer (50 mM NaH_2PO_4, 30 mM NaCl, and 250 mM imidazole, pH 7.4).

For GST-tagged proteins, the pellet was resuspended in 1× PBS (150 mM NaCl, 10 mM Na_2HPO_4, 2 mM KH_2PO_4, 2.7 mM KCl, pH 7.4, 1 mM PMSF, and 1× cocktail) and sonicated for 10 min. After centrifugation for 30 min at 7000*g* and 4°C, the supernatant was incubated with Glutathione Sepharose 4B (GE) resin for 3 h at 4°C. The resin was washed three times with 1× PBS to remove nonspecifically bound proteins. The GST-tagged proteins were eluted from the resin with GSH buffer (50 mM Tris-HCl, pH 8.0, and 10 mM GSH).

For MBP-tagged proteins, the pellet was resuspended in lysis buffer (20 mM Tris-HCl, pH 7.4, 200 mM NaCl, 1 mM EDTA, 1 mM PMSF, and 1× cocktail) and sonicated for 10 min. After centrifugation for 30 min at 7000*g* and 4°C, the supernatant was incubated with amylose resin (NEB) for 3 h at 4°C. The resin was washed three times with lysis buffer to remove nonspecifically bound proteins. The MBP-tagged proteins were eluted from the resin with elution buffer (20 mM Tris-HCl, pH 7.4, 200 mM NaCl, 1 mM EDTA, and 10 mM maltose).

The purified proteins were mixed with Quick Start Bradford 1× Dye Reagent (Bio-Rad), and the absorbance was measured at 595 nm. Protein concentrations were calculated based on a standard curve with BSA as a substrate.

Protein Pull-Down Assay

The pull-down assay was performed as described (Ding et al., 2015) with some modifications. In brief, the corresponding CDS of *EAR1*$^{121\text{-}287}$, *ABI1*, or *ABI2* was cloned into the pET-30a (+) vector or the pMAL-c5X vector. EAR1$^{121\text{-}287}$-His protein was purified on Ni Sepharose (GE), and MBP, MBP-ABI1, or MBP-ABI2 was purified on amylose resin (NEB). Purified MBP, MBP-ABI1, or MBP-ABI2 protein (10 μg) was incubated with amylose resin for 2 h in a tube with pull-down binding buffer (150 mM NaCl, 10 mM Na_2HPO_4, 2 mM KH_2PO_4, 2.7 mM KCl, and 0.1% Nonidet P-40, pH 7.4) at 4°C. After a brief centrifugation at 1000*g* for 3 min at 4°C, the buffer was removed and 2 μg of EAR1$^{121\text{-}287}$-His protein was added to the resin, along with fresh binding buffer. The tube was rotated at 4°C for 2 h for protein binding. The resin was washed five times with 1× PBS (150 mM NaCl, 10 mM Na_2HPO_4, 2 mM KH_2PO_4, and 2.7 mM KCl, pH 7.4) to remove nonspecifically bound protein, combined with 50 μL of 1× PBS and 10 μL of 6× SDS loading buffer, and boiled for 5 min. After centrifugation at 12,000*g* for 1 min at 22°C, the supernatant was subjected to immunoblotting analysis.

For HAB1, HAB2, AHG1, and AHG3, the corresponding CDS was cloned into pET-28a (+) (for HAB1) or pET-30a (+) (the others) (with His tag), and the proteins were purified on Ni Sepharose (GE). The CDS of *EAR1*$^{121\text{-}287}$ was cloned into pGEX-4T-1 (with GST tag), and the proteins were purified on Glutathione Sepharose 4B beads (GE). Subsequently, 10 μg of GST or GST-EAR1 proteins was incubated with Glutathione Sepharose 4B beads for 2 h with pull-down binding buffer at 4°C. The buffer was removed, and 2 μg of HAB1-His, HAB2-His, AHG1-His, or AHG3-His protein was combined with fresh binding buffer and rotated at 4°C for 2 h. The beads were washed five times with washing buffer, combined with 50 μL of 1× PBS and 10 μL of 6×SDS loading buffer, and boiled for 5 min. The supernatant was used for immunoblotting analysis.

Co-IP and LC-MS/MS Assay

The co-IP assay was performed using Arabidopsis protoplasts as described previously (Kong et al., 2015). Briefly, the full-length CDS of *EAR1*, *ABI1*, *ABI2*, *HAB1*, *HAB2*, *AHG1*, and *AHG3* were cloned into the pCAMBIA1300 vector and fused to a Myc or Flag tag. The *Pro35S:EAR1-Flag* constructs were cotransformed into Arabidopsis mesophyll protoplasts along with *Pro35S:ABI1-Myc*, *Pro35S:ABI2-Myc*, *Pro35S:HAB1-Myc*, *Pro35S:HAB2-Myc*, *Pro35S:AHG1-Myc*, and *Pro35S:AHG3-Myc*. After incubation for 14 to 16 h, total proteins were extracted from the protoplasts, and the extracts were incubated with anti-c-Myc-Agarose Affinity Gel (Sigma-Aldrich) at 4°C for 3 h. The beads were washed five times with PBS (pH 7.5) and boiled for 5 min in 6× SDS loading buffer. After centrifugation at 12,000*g* for 1 min, the supernatants were used for immunoblotting analysis.

Transgenic plants harboring *Pro35S:EAR1-Flag* (*OE-16*$^{\#}$) were also subjected to co-IP assays as described previously with some modifications (Gao et al., 2015). Briefly, total proteins were extracted from the wild type and *OE-16*$^{\#}$ with immunoprecipitation buffer (150 mM NaCl, 10 mM Tris-HCl, pH 7.6, 2 mM EDTA, 0.5% Nonidet P-40, and 1× protease inhibitor [Roche]) and incubated with anti-Flag M2 Affinity gel (Sigma-Aldrich) at 4°C for 3 h. The beads were subsequently washed five times with PBS (pH 7.5) at 4°C for 10 min each time. After centrifugation at 1000*g* for 3 min, the beads were boiled for 5 min in 100 μL of PBS and 20 μL of 6× SDS loading buffer. The immunoprecipitated proteins were used for immunoblotting analysis, in which the ABI1 and ABI2 proteins were detected using anti-ABI1 and anti-ABI2 antibodies, respectively, and the EAR1 proteins were detected using an anti-Flag antibody (Sigma-Aldrich, F1804) as a loading control. The ABI2 polyclonal antibodies were produced by Beijing Protein Innovation. Briefly, a *Bgl*II/*Eco*RI fragment containing the full-length *ABI2* open reading frame was cloned into the *Bam*HI/*Eco*RI sites of the pET-28a vector to express 6× His-tagged ABI2 protein. The fusion protein was expressed in *E. coli*, purified, and used as an antigen to immunize rabbits for the production of polyclonal antiserum. Antigen affinity-purified anti-ABI2 antibodies were used in immunoblot analysis. The specificity of the ABI2 antibodies was checked by comparing the *abi2-2* mutant with the wild type (Supplemental Figure 4). The immunoprecipitated proteins were also used for LC-MS/MS analysis on a Thermo Q-Exactive high-resolution mass spectrometer (Thermo Scientific) as described previously (Kong et al., 2015).

BiFC Assay

BiFC assays were performed as described previously (Waadt and Kudla, 2008). Briefly, the full-length CDS of *EAR1* was cloned into the pSPYCE(M) vector to generate the EAR1-cYFP plasmid, and *ABI1*, *ABI2*, *HAB11*, *HAB2*, *AHG1*, and *AHG3* were cloned into the pSPYNE173 vector to construct the ABI1-nYFP, ABI2-nYFP, HAB1-nYFP, HAB2-nYFP, AHG1-nYFP, and AHG3-nYFP plasmids, respectively. To produce truncated EAR1 and ABI1, the corresponding CDS of *EAR1* and *ABI1* were amplified and cloned into the pSPYCE(M) and pSPYNE173 vectors, forming the EAR1$^{1\text{-}287}$-cYFP, EAR1$^{1\text{-}120}$-cYFP, EAR1$^{121\text{-}287}$-cYFP, EAR1$^{191\text{-}287}$-cYFP, EAR1$^{191\text{-}270}$-cYFP, EAR1$^{288\text{-}463}$-cYFP, ABI1$^{1\text{-}120}$-nYFP, ABI1$^{1\text{-}130}$-nYFP, and ABI1$^{131\text{-}434}$-nYFP constructs. The plasmids were then transformed into Agrobacterium GV3101 cells, and different combinations were mixed for injection into *Nicotiana benthamiana* leaves with the silencing suppressor P19 strain. The plants were grown at 18°C under a 12-h-light/12-h-dark cycle in a greenhouse for 48 to 72 h, and YFP signals were observed under a confocal laser-scanning microscope (Zeiss LSM 510 META).

Yeast Three-Hybrid Assay

The yeast three-hybrid assay was performed as described previously (Ding et al., 2015). In brief, the plasmids (pGADT7-ABI1 and pBridge-PYR1 or pGADT7-ABI1 and pBridge-PYR1-EAR1) were cotransformed into yeast strain AH109. Positive clones were selected on synthetic complete medium lacking Leu, Trp, Ade, and Met. β-Galactosidase activity was

Downloaded from https://academic.oup.com/plcell/article/30/4/815/6099023 by guest on 21 August 2022

measured using a Yeast β-Galactosidase Assay Kit (product 75768, Thermo Scientific) following the manufacturer's instructions. Ten positive clones were used for the β-galactosidase activity assay in each experiment. Three independent experiments were performed, with similar results.

Cell Fractionation Assay

Cell fractionation assays were performed as described previously (Wang et al., 2011b). Briefly, 0.5-g samples of 2-week-old *OE-16#* transgenic plants were ground in liquid nitrogen and mixed with 2 mL of fractionation lysis buffer (20 mM Tris-HCl, pH 7.5, 25% glycerol, 2 mM EDTA, 2.5 mM $MgCl_2$, 20 mM KCl, 250 mM sucrose, with the addition of 5 mM DTT with 1× protease inhibitor cocktail [Roche] before use). The mixture was vortexed and filtered through a double layer of Miracloth (Millipore). The flow-through was centrifuged at 1500*g* for 10 min at 4°C, after which the supernatant was centrifuged at 10,000*g* for 10 min at 4°C, and the pellet was collected as the cytoplasmic fraction. The pellet from the first centrifugation was washed five times or more with NRBT buffer (20 mM Tris-HCl, pH 7.5, 25% glycerol, 2.5 mM $MgCl_2$, and 0.2% Triton X-100) until it turned oyster white. The pellet was resuspended in 400 μL of NRB2 (20 mM Tris-HCl, pH 7.5, 0.25 M sucrose, 10 mM $MgCl_2$, 0.5% Triton X-100, and 5 mM β-mercaptoethanol supplemented with 1× protease inhibitor cocktail) and added on top of a layer of 400 μL of NRB3 (20 mM Tris-HCl, pH 7.5, 1.7 M sucrose, 10 mM $MgCl_2$, 0.5% Triton X-100, and 5 mM β-mercaptoethanol supplemented with 1× protease inhibitor cocktail). The suspension was centrifuged at 16,000*g* for 45 min at 4°C, and the pellet was collected as the nuclear fraction. Both the cytoplasmic and nuclear fractions were resuspended in 2× SDS loading buffer and boiled for 5 min for the immunoblot assays. EAR1 proteins were detected using an anti-Flag antibody (Sigma-Aldrich, F1804). Tubulin was detected with an anti-tubulin antibody (Sigma-Aldrich, T3526) as a cytoplasmic marker (Saslowsky et al., 2005). H3 proteins were detected using an anti-H3 antibody (Millipore, 17-10046) as a nuclear marker (Feys et al., 2005).

The microsomal fractionation assay was performed as described previously (Bueso et al., 2014). In brief, 0.1-g samples of 2-week-old *OE-16#* transgenic plants were ground in liquid nitrogen and mixed with 800 μL of LE buffer (80 mM Tris-HCl, pH 7.5, 12% sucrose, 1 mM EDTA, 1 mM DTT, 1 mM PMSF, and 5 mg/mL leupeptin). The crude extract was centrifuged at 10,000*g* for 10 min at 4°C, and the supernatant was collected as total protein. The supernatant was centrifuged at 100,000*g* for 1 h, and the new supernatant was collected as the soluble fraction; the pellet was resuspended in LE buffer and collected as the microsomal fraction. Both fractions were analyzed by immunoblotting, and EAR1 proteins were detected using an anti-Flag antibody (Sigma-Aldrich).

Measurement of PP2C Activity

PP2C activity was measured using a Ser/Thr Phosphatase Assay Kit (Promega) as described previously (Yu et al., 2012). In brief, the corresponding CDS of *ABI1*, *ABI2*, *HAB1*, *HAB2*, *AHG1*, *AHG3*, $EAR1^{121\text{-}287}$, $EAR1^{191\text{-}287}$, $EAR1^{121\text{-}210}$, $EAR1^{201\text{-}287}$, $EAR1^{191\text{-}260}$, and $EAR1^{191\text{-}270}$ were fused with the pET-28a (+) (for *HAB1*) or pET-30a (+) (the others) vectors, and the constructs were transformed into the *E. coli* strain BL21. The recombinant proteins were purified on Ni Sepharose (GE) and eluted with elution buffer (50 mM Tris-HCl, pH 7.2, and 250 mM imidazole). None of the buffers used for protein purification contained phosphate. To measure phosphatase activity, different combinations of EAR1 truncated proteins and PP2C proteins were mixed with 5 μL of 1 mM phosphopeptide [RRA(phosphoT)VA] and 10 μL of PP2C 5× reaction buffer (250 mM imidazole, pH 7.2, 1 mM EGTA, 25 mM $MgCl_2$, 0.1% β-mercaptoethanol, and 0.5 mg/mL BSA) at 25°C for 15 min. The reactions were stopped by adding 50 μL of molybdate dye/additive mixture, and the plate was incubated at room temperature for 15 min. The absorbance was measured at 630 nm in a Microplate Reader (Power Wave XS2). As $EAR1^{121\text{-}210}$, $EAR1^{201\text{-}287}$, $EAR1^{191\text{-}260}$, and $EAR1^{191\text{-}270}$ did not enhance PP2C activity, they were considered to serve as controls.

To measure PP2C activity in lysates, total proteins (0.1 g) from the wild type, *ear1-1*, *OE-16#*, *OE-28#*, *3m*, and *4m* were extracted in phosphatase storage buffer (20 mM Tris-HCl, pH 7.5, 20 mM KCl, 1 mM EDTA, 1 mM EGTA, 10 mM DTT, 0.5% Triton X-100, and 50% glycerol) with 1× protease inhibitor cocktail (Roche), and the homogenized lysate was centrifuged at 100,000*g* for 60 min at 4°C. The supernatant was passed through Sephadex G-25 resin to remove the endogenous phosphates in the tissue extract, and the filtered lysate was used to measure PP2C activity as described above but with the addition of 5 μM okadaic acid.

In Vitro Phosphorylation Assay

The in vitro phosphorylation assay was performed as described previously (Ding et al., 2015). In brief, the corresponding CDS of *OST1*, *ABI1*, and $EAR1^{121\text{-}287}$ were fused with the pET-30a (+) vector (Novagen). The correct plasmids were transformed into *E. coil* BL21 (DE3) cells, and the recombinant proteins were purified on Ni Sepharose (GE). The in vitro phosphorylation assay was performed using 4 μg of OST1-His with different combinations of ABI1-His and $EAR1^{121\text{-}287}$-His recombinant proteins. The mixed proteins were incubated in kinase buffer (100 mM HEPES-NaOH, pH 7.5, 10 mM $MgCl_2$, 2 mM DTT, and 0.5 mM ATP) with 2 μCi of [γ-^{32}P]ATP in a 20-μL volume at 30°C for 20 min. The reactions were stopped by adding 4 μL of 6× SDS loading buffer, and the proteins were separated by 10% SDS-PAGE. The gel was washed three times with distilled water, and radioactivity in the autoradiograph was detected using X-OMAT BT Film (Carestream) or a Typhoon 9410 imager.

In-Gel Kinase Assay

The in-gel kinase assay was performed as described previously (Kong et al., 2015). In brief, total proteins were extracted from the wild type, *OE-16#*, *ear1*, and *ost1* with lysis buffer (50 mM HEPES-KOH, pH 7.5, 5 mM EDTA, 5 mM EGTA, 2 mM DTT, 25 mM NaF, 1 mM Na_3VO_4, 20% glycerol, and 1× protease inhibitor cocktail [Roche]). Total proteins (80 μg) were separated on an SDS-PAGE gel containing 0.1 mg/mL GST-Δ(73-118) substrate and washed three times with SDS removing buffer (25 mM Tris-HCl, pH 7.5, 0.5 mM DTT, 5 mM NaF, 0.1 mM Na_3VO_4, 0.5 mg/mL BSA, and 0.1% Triton X-100) at room temperature for 20 min each time. The gel was then washed three times with renaturing buffer (25 mM Tris-HCl, pH 7.5, 1 mM DTT, 5 mM NaF, and 0.1 mM Na_3VO_4) for 1, 12, and 1 h at 4°C to renature the proteins in the gel. After incubation in kinase reaction buffer (40 mM HEPES-KOH, pH 7.5, 1 mM DTT, 2 mM EGTA, 12 mM $MgCl_2$, and 0.1 mM Na_3VO_4) for 30 min, the gel was incubated in 30 mL of fresh kinase reaction buffer with 60 μCi of [γ-^{32}P]ATP and 9 μL of 1 mM cold ATP at room temperature for 3 h. Finally, the gel was washed five times with 5% trichloroacetic acid and 1% sodium pyrophosphate for 30 min each time. The gel was covered with a storage phosphor screen (GE), and radioactivity was detected with a Typhoon 9410 imager.

The primers used in this study are listed in the Supplemental Data Set 3.

Accession Numbers

Sequence data from this article can be found in the GenBank/EMBL data libraries under the following accession numbers: *EAR1*, *At5g22090*; *ABI1*, *At4g26080*; *ABI2*, *At5g57050*; *HAB1*, *At1g72770*; *HAB2*, *At1g17550*; *AHG1*, *At5g51760*; *AHG3*, *At3g11410*; *HAI1*, *At5g59220*; *HAI2*, *At1g07430*; *HAI3*, *At2g29380*; *SnRK2.6/OST1*, *At4g33950*; *RD29A*, *At5g52310*; *RD29B*, *At5g52300*; *RAB18*, *At1g43890*; *ABF4*, *At3g19290*; *P5CS1*, *At2g39800*; and *KIN1*, *At1g14370*. Mutants used in this article can be obtained from the ABRC under the following accession numbers: *ear1-2*

Downloaded from https://academic.oup.com/plcell/article/30/4/815/6099023 by guest on 21 August 2022

(SALK_057606), *abi1-2* (SALK_072009), *abi2-2* (SALK_015166), *hab1-1* (SALK_002104), *ost1/snrk2.6* (SALK_008068), *snrk2.2* (GABI-Kat 807G04), and *snrk2.3* (SALK_107315).

Supplemental Data

Supplemental Figure 1. Phenotypes of *SALK_057606* (*ear1-2*) and *ear1-c* Mutants.

Supplemental Figure 2. Phylogenetic Analysis of EAR1 Sequences.

Supplemental Figure 3. Comparison of Plant Phenotypes among the Wild Type, *ear1-1*, and EAR1-Overexpressing Lines *OE-16*$^{\#}$ and *OE-28*$^{\#}$.

Supplemental Figure 4. EAR1 Interacts with Clade A PP2Cs.

Supplemental Figure 5. EAR1 Enhances the Activity of the Clade A PP2Cs.

Supplemental Figure 6. EAR1 Does Not Influence the Interaction between ABI1 and PYR1 or the Degradation of ABI1.

Supplemental Figure 7. Protein Characteristics of EAR1 and PP2Cs.

Supplemental Figure 8. EAR1 Negatively Regulates the Expression of ABA-Inducible Genes.

Supplemental Figure 9. Subcellular Localization of EAR1.

Supplemental Data Set 1. Alignments Use to Generate the Phylogeny Presented in Supplemental Figure 2A.

Supplemental Data Set 2. LC-MS/MS Results for EAR1 Interaction Proteins without ABA Treatment in Arabidopsis.

Supplemental Data Set 3. LC-MS/MS Results for EAR1 Interaction Proteins with ABA Treatment in Arabidopsis.

Supplemental Data Set 4. Primers Used in This Study.

ACKNOWLEDGMENTS

We thank Zhen Li at China Agricultural University for performing LC-MS/MS analysis. This work was supported by grants from the National Major Project for Transgenic Organism Breeding (Ministry of Agriculture and Rural Affairs of the People's Republic of China) (2016ZX08009002) and the National Basic Research Program of China (2012CB114300).

AUTHOR CONTRIBUTIONS

Z.G., K.W., and J.H. conceived the study and designed experiments. K.W. and J.H. performed the main experiments. Y.Z. performed the transient assays for *ProRD29B:LUC*. J.L. produced the ABI2 antibodies and performed immunoblotting analyses. Z.G., K.W., and J.H. wrote the manuscript. All other authors discussed the results and commented on the manuscript.

Received November 14, 2017; revised February 8, 2018; accepted April 2, 2018; published April 4, 2018.

REFERENCES

Bhaskara, G.B., Nguyen, T.T., and Verslues, P.E. (2012). Unique drought resistance functions of the highly ABA-induced clade A protein phosphatase 2Cs. Plant Physiol. **160:** 379–395.

Brandt, B., Brodsky, D.E., Xue, S., Negi, J., Iba, K., Kangasjärvi, J., Ghassemian, M., Stephan, A.B., Hu, H., and Schroeder, J.I. (2012). Reconstitution of abscisic acid activation of SLAC1 anion channel by CPK6 and OST1 kinases and branched ABI1 PP2C phosphatase action. Proc. Natl. Acad. Sci. USA **109:** 10593–10598.

Brandt, B., Munemasa, S., Wang, C., Nguyen, D., Yong, T., Yang, P.G., Poretsky, E., Belknap, T.F., Waadt, R., Aleman, F., and Schroeder, J.I. (2015). Calcium specificity signaling mechanisms in abscisic acid signal transduction in Arabidopsis guard cells. eLife **4:** e03599.

Bueso, E., Rodriguez, L., Lorenzo-Orts, L., Gonzalez-Guzman, M., Sayas, E., Muñoz-Bertomeu, J., Ibañez, C., Serrano, R., and Rodriguez, P.L. (2014). The single-subunit RING-type E3 ubiquitin ligase RSL1 targets PYL4 and PYR1 ABA receptors in plasma membrane to modulate abscisic acid signaling. Plant J. **80:** 1057–1071.

Chen, J.W., Zhang, Q., Li, X.S., and Cao, K.F. (2011). Steady and dynamic photosynthetic responses of seedlings from contrasting successional groups under low-light growth conditions. Physiol. Plant. **141:** 84–95.

Clough, S.J., and Bent, A.F. (1998). Floral dip: a simplified method for Agrobacterium-mediated transformation of *Arabidopsis thaliana*. Plant J. **16:** 735–743.

Cutler, S.R., Rodriguez, P.L., Finkelstein, R.R., and Abrams, S.R. (2010). Abscisic acid: emergence of a core signaling network. Annu. Rev. Plant Biol. **61:** 651–679.

Ding, Y., Li, H., Zhang, X., Xie, Q., Gong, Z., and Yang, S. (2015). OST1 kinase modulates freezing tolerance by enhancing ICE1 stability in Arabidopsis. Dev. Cell **32:** 278–289.

Disfani, F.M., Hsu, W.L., Mizianty, M.J., Oldfield, C.J., Xue, B., Dunker, A.K., Uversky, V.N., and Kurgan, L. (2012). MoRFpred, a computational tool for sequence-based prediction and characterization of short disorder-to-order transitioning binding regions in proteins. Bioinformatics **28:** i75–i83.

Eto, M., and Brautigan, D.L. (2012). Endogenous inhibitor proteins that connect Ser/Thr kinases and phosphatases in cell signaling. IUBMB Life **64:** 732–739.

Feys, B.J., Wiermer, M., Bhat, R.A., Moisan, L.J., Medina-Escobar, N., Neu, C., Cabral, A., and Parker, J.E. (2005). Arabidopsis SENESCENCE-ASSOCIATED GENE101 stabilizes and signals within an ENHANCED DISEASE SUSCEPTIBILITY1 complex in plant innate immunity. Plant Cell **17:** 2601–2613.

Fujii, H., Verslues, P.E., and Zhu, J.K. (2007). Identification of two protein kinases required for abscisic acid regulation of seed germination, root growth, and gene expression in Arabidopsis. Plant Cell **19:** 485–494.

Fujii, H., Chinnusamy, V., Rodrigues, A., Rubio, S., Antoni, R., Park, S.Y., Cutler, S.R., Sheen, J., Rodriguez, P.L., and Zhu, J.K. (2009). In vitro reconstitution of an abscisic acid signalling pathway. Nature **462:** 660–664.

Furihata, T., Maruyama, K., Fujita, Y., Umezawa, T., Yoshida, R., Shinozaki, K., and Yamaguchi-Shinozaki, K. (2006). Abscisic acid-dependent multisite phosphorylation regulates the activity of a transcription activator AREB1. Proc. Natl. Acad. Sci. USA **103:** 1988–1993.

Gao, M.J., et al. (2015). SCARECROW-LIKE15 interacts with HISTONE DEACETYLASE19 and is essential for repressing the seed maturation programme. Nat. Commun. **6:** 7243.

Geiger, D., Scherzer, S., Mumm, P., Stange, A., Marten, I., Bauer, H., Ache, P., Matschi, S., Liese, A., Al-Rasheid, K.A., Romeis, T., and Hedrich, R. (2009). Activity of guard cell anion channel SLAC1 is controlled by drought-stress signaling kinase-phosphatase pair. Proc. Natl. Acad. Sci. USA **106:** 21425–21430.

Geiger, D., Scherzer, S., Mumm, P., Marten, I., Ache, P., Matschi, S., Liese, A., Wellmann, C., Al-Rasheid, K.A., Grill, E., Romeis, T., and Hedrich, R. (2010). Guard cell anion channel SLAC1 is

Downloaded from https://academic.oup.com/plcell/article/30/4/815/6099023 by guest on 21 August 2022

regulated by CDPK protein kinases with distinct Ca^{2+} affinities. Proc. Natl. Acad. Sci. USA **107:** 8023–8028.

Hao, Q., Yin, P., Li, W., Wang, L., Yan, C., Lin, Z., Wu, J.Z., Wang, J., Yan, S.F., and Yan, N. (2011). The molecular basis of ABA-independent inhibition of PP2Cs by a subclass of PYL proteins. Mol. Cell **42:** 662–672.

He, J., Duan, Y., Hua, D., Fan, G., Wang, L., Liu, Y., Chen, Z., Han, L., Qu, L.J., and Gong, Z. (2012). DEXH box RNA helicase-mediated mitochondrial reactive oxygen species production in Arabidopsis mediates crosstalk between abscisic acid and auxin signaling. Plant Cell **24:** 1815–1833.

Hua, D., Wang, C., He, J., Liao, H., Duan, Y., Zhu, Z., Guo, Y., Chen, Z., and Gong, Z. (2012). A plasma membrane receptor kinase, GHR1, mediates abscisic acid- and hydrogen peroxide-regulated stomatal movement in Arabidopsis. Plant Cell **24:** 2546–2561.

Irigoyen, M.L., et al. (2014). Targeted degradation of abscisic acid receptors is mediated by the ubiquitin ligase substrate adaptor DDA1 in Arabidopsis. Plant Cell **26:** 712–728.

Kerk, D., Templeton, G., and Moorhead, G.B.G. (2008). Evolutionary radiation pattern of novel protein phosphatases revealed by analysis of protein data from the completely sequenced genomes of humans, green algae, and higher plants. Plant Physiol. **146:** 351–367.

Kong, L., Cheng, J., Zhu, Y., Ding, Y., Meng, J., Chen, Z., Xie, Q., Guo, Y., Li, J., Yang, S., and Gong, Z. (2015). Degradation of the ABA co-receptor ABI1 by PUB12/13 U-box E3 ligases. Nat. Commun. **6:** 8630.

Koornneef, M., Reuling, G., and Karssen, C.M. (1984). The isolation and characterization of abscisic acid-insensitive mutants of *Arabidopsis thaliana*. Physiol. Plant. **61:** 377–383.

Leung, J., Bouvier-Durand, M., Morris, P.C., Guerrier, D., Chefdor, F., and Giraudat, J. (1994). Arabidopsis ABA response gene ABI1: features of a calcium-modulated protein phosphatase. Science **264:** 1448–1452.

Leung, J., Merlot, S., and Giraudat, J. (1997). The Arabidopsis ABSCISIC ACID-INSENSITIVE2 (ABI2) and ABI1 genes encode homologous protein phosphatases 2C involved in abscisic acid signal transduction. Plant Cell **9:** 759–771.

Li, J., Shi, C., Sun, D., He, Y., Lai, C., Lv, P., Xiong, Y., Zhang, L., Wu, F., and Tian, C. (2015). The HAB1 PP2C is inhibited by ABA-dependent PYL10 interaction. Sci. Rep. **5:** 10890.

Li, Y., Zhang, L., Li, D., Liu, Z., Wang, J., Li, X., and Yang, Y. (2016). The Arabidopsis F-box E3 ligase RIFP1 plays a negative role in abscisic acid signalling by facilitating ABA receptor RCAR3 degradation. Plant Cell Environ. **39:** 571–582.

Lillo, C., Kataya, A.R., Heidari, B., Creighton, M.T., Nemie-Feyissa, D., Ginbot, Z., and Jonassen, E.M. (2014). Protein phosphatases PP2A, PP4 and PP6: mediators and regulators in development and responses to environmental cues. Plant Cell Environ. **37:** 2631–2648.

Liu, L., Cui, F., Li, Q., Yin, B., Zhang, H., Lin, B., Wu, Y., Xia, R., Tang, S., and Xie, Q. (2011). The endoplasmic reticulum-associated degradation is necessary for plant salt tolerance. Cell Res. **21:** 957–969.

Melcher, K., et al. (2009). A gate-latch-lock mechanism for hormone signalling by abscisic acid receptors. Nature **462:** 602–608.

Mészáros, B., Simon, I., and Dosztányi, Z. (2009). Prediction of protein binding regions in disordered proteins. PLOS Comput. Biol. **5:** e1000376.

Meyer, K., Leube, M.P., and Grill, E. (1994). A protein phosphatase 2C involved in ABA signal transduction in Arabidopsis thaliana. Science **264:** 1452–1455.

Miyazono, K., et al. (2009). Structural basis of abscisic acid signalling. Nature **462:** 609–614.

Nishimura, N., Yoshida, T., Kitahata, N., Asami, T., Shinozaki, K., and Hirayama, T. (2007). ABA-Hypersensitive Germination1 encodes a protein phosphatase 2C, an essential component of abscisic acid signaling in Arabidopsis seed. Plant J. **50:** 935–949.

Park, S.Y., et al. (2009). Abscisic acid inhibits type 2C protein phosphatases via the PYR/PYL family of START proteins. Science **324:** 1068–1071.

Rodriguez, P.L., Benning, G., and Grill, E. (1998). ABI2, a second protein phosphatase 2C involved in abscisic acid signal transduction in Arabidopsis. FEBS Lett. **421:** 185–190.

Rubio, S., Rodrigues, A., Saez, A., Dizon, M.B., Galle, A., Kim, T.H., Santiago, J., Flexas, J., Schroeder, J.I., and Rodriguez, P.L. (2009). Triple loss of function of protein phosphatases type 2C leads to partial constitutive response to endogenous abscisic acid. Plant Physiol. **150:** 1345–1355.

Santiago, J., Dupeux, F., Round, A., Antoni, R., Park, S.Y., Jamin, M., Cutler, S.R., Rodriguez, P.L., and Márquez, J.A. (2009). The abscisic acid receptor PYR1 in complex with abscisic acid. Nature **462:** 665–668.

Saslowsky, D.E., Warek, U., and Winkel, B.S.J. (2005). Nuclear localization of flavonoid enzymes in Arabidopsis. J. Biol. Chem. **280:** 23735–23740.

Sheen, J. (1998). Mutational analysis of protein phosphatase 2C involved in abscisic acid signal transduction in higher plants. Proc. Natl. Acad. Sci. USA **95:** 975–980.

Shi, Y. (2009). Serine/threonine phosphatases: mechanism through structure. Cell **139:** 468–484.

Soon, F.F., et al. (2012). Molecular mimicry regulates ABA signaling by SnRK2 kinases and PP2C phosphatases. Science **335:** 85–88.

Sun, X., Rikkerink, E.H., Jones, W.T., and Uversky, V.N. (2013). Multifarious roles of intrinsic disorder in proteins illustrate its broad impact on plant biology. Plant Cell **25:** 38–55.

Takemiya, A., Ariyoshi, C., and Shimazaki, K. (2009). Identification and functional characterization of inhibitor-3, a regulatory subunit of protein phosphatase 1 in plants. Plant Physiol. **150:** 144–156.

Templeton, G.W., Nimick, M., Morrice, N., Campbell, D., Goudreault, M., Gingras, A.C., Takemiya, A., Shimazaki, K., and Moorhead, G.B. (2011). Identification and characterization of Atl-2, an Arabidopsis homologue of an ancient protein phosphatase 1 (PP1) regulatory subunit. Biochem. J. **435:** 73–83.

Tischer, S.V., Wunschel, C., Papacek, M., Kleigrewe, K., Hofmann, T., Christmann, A., and Grill, E. (2017). Combinatorial interaction network of abscisic acid receptors and coreceptors from *Arabidopsis thaliana*. Proc. Natl. Acad. Sci. USA **114:** 10280–10285.

Umezawa, T., Sugiyama, N., Mizoguchi, M., Hayashi, S., Myouga, F., Yamaguchi-Shinozaki, K., Ishihama, Y., Hirayama, T., and Shinozaki, K. (2009). Type 2C protein phosphatases directly regulate abscisic acid-activated protein kinases in Arabidopsis. Proc. Natl. Acad. Sci. USA **106:** 17588–17593.

Vlad, F., Rubio, S., Rodrigues, A., Sirichandra, C., Belin, C., Robert, N., Leung, J., Rodriguez, P.L., Laurière, C., and Merlot, S. (2009). Protein phosphatases 2C regulate the activation of the Snf1-related kinase OST1 by abscisic acid in Arabidopsis. Plant Cell **21:** 3170–3184.

Waadt, R., and Kudla, J. (2008). In planta visualization of protein interactions using bimolecular fluorescence complementation (BiFC). CSH Protoc. **2008:** pdb.prot4995.

Walter, M., Chaban, C., Schütze, K., Batistic, O., Weckermann, K., Näke, C., Blazevic, D., Grefen, C., Schumacher, K., Oecking, C., Harter, K., and Kudla, J. (2004). Visualization of protein interactions in

Downloaded from https://academic.oup.com/plcell/article/30/4/815/6099023 by guest on 21 August 2022

living plant cells using bimolecular fluorescence complementation. Plant J. **40:** 428–438.

Wang, L., Hua, D., He, J., Duan, Y., Chen, Z., Hong, X., and Gong, Z. (2011a). Auxin Response Factor2 (ARF2) and its regulated homeodomain gene HB33 mediate abscisic acid response in Arabidopsis. PLoS Genet. **7:** e1002172.

Wang, Z., Meng, P., Zhang, X., Ren, D., and Yang, S. (2011b). BON1 interacts with the protein kinases BIR1 and BAK1 in modulation of temperature-dependent plant growth and cell death in Arabidopsis. Plant J. **67:** 1081–1093.

Wang, Z.P., Xing, H.L., Dong, L., Zhang, H.Y., Han, C.Y., Wang, X.C., and Chen, Q.J. (2015). Egg cell-specific promoter-controlled CRISPR/Cas9 efficiently generates homozygous mutants for multiple target genes in Arabidopsis in a single generation. Genome Biol. **16:** 144.

Yang, J., Roe, S.M., Cliff, M.J., Williams, M.A., Ladbury, J.E., Cohen, P.T., and Barford, D. (2005). Molecular basis for TPR domain-mediated regulation of protein phosphatase 5. EMBO J. **24:** 1–10.

Yin, P., Fan, H., Hao, Q., Yuan, X., Wu, D., Pang, Y., Yan, C., Li, W., Wang, J., and Yan, N. (2009). Structural insights into the mechanism of abscisic acid signaling by PYL proteins. Nat. Struct. Mol. Biol. **16:** 1230–1236.

Yoshida, T., Nishimura, N., Kitahata, N., Kuromori, T., Ito, T., Asami, T., Shinozaki, K., and Hirayama, T. (2006). ABA-hypersensitive germination3 encodes a protein phosphatase 2C (AtPP2CA) that strongly regulates abscisic acid signaling during germination among Arabidopsis protein phosphatase 2Cs. Plant Physiol. **140:** 115–126.

Yu, F., et al. (2012). FERONIA receptor kinase pathway suppresses abscisic acid signaling in Arabidopsis by activating ABI2 phosphatase. Proc. Natl. Acad. Sci. USA **109:** 14693–14698.

Zhao, J., Zhao, L., Zhang, M., Zafar, S.A., Fang, J., Li, M., Zhang, W., and Li, X. (2017). Arabidopsis E3 ubiquitin ligases PUB22 and PUB23 negatively regulate drought tolerance by targeting ABA receptor PYL9 for degradation. Int. J. Mol. Sci. **18:** E1841.

Downloaded from https://academic.oup.com/plcell/article/30/4/815/6099023 by guest on 21 August 2022